



# **BRNO UNIVERSITY OF TECHNOLOGY**

VYSOKÉ UČENÍ TECHNICKÉ V BRNĚ

## **FACULTY OF MECHANICAL ENGINEERING**

FAKULTA STROJNÍHO INŽENÝRSTVÍ

## **INSTITUTE OF PROCESS ENGINEERING**

ÚSTAV PROCESNÍHO INŽENÝRSTVÍ

# **THE INFLUENCE OF THE COMBUSTION AIR TEMPERATURE ON PARAMETERS OF THE COMBUSTION PROCESS**

VLIV TEPLoty SPALOVACÍHO VZDUCHU NA PARAMETRY SPALOVACÍHO PROCESU

## **MASTER'S THESIS**

DIPLOMOVÁ PRÁCE

### **AUTHOR**

AUTOR PRÁCE

**Bc. Radek Šimeček**

### **SUPERVISOR**

VEDOUCÍ PRÁCE

**Ing. Pavel Skryja, Ph.D.**

**BRNO, 2019**

# Master's Thesis Assignment

Institut: Institute of Process Engineering  
Student: **Bc. Radek Šimeček**  
Degree programm: Mechanical Engineering  
Branch: Process Engineering  
Supervisor: **Ing. Pavel Skryja, Ph.D.**  
Academic year: 2018/19

As provided for by the Act No. 111/98 Coll. on higher education institutions and the BUT Study and Examination Regulations, the director of the Institute hereby assigns the following topic of Master's Thesis:

## **The influence of the combustion air temperature on parameters of the combustion process**

### **Brief description:**

Industrial applications acquire the necessary energy by combusting gaseous, liquid or solid fuels. Thermal energy is needed in applications such as heating process substances (water, oil, etc.) or processing solid materials (metallic, non-metallic, glass sand, etc.). The emissions of nitrogen oxides (NO<sub>x</sub>) and carbon monoxide (CO) are the most significant. Other emissions present in the flue gases can be sulphur oxides, solid pollutants, volatile substances, etc. For this reason, stationary combustion sources are strictly required to comply with the emission limits. Complying with the emission limits is often complicated, especially in conditions where preheated combustion air is used, because preheated air increase NO<sub>x</sub> formation.

The aim of this works is to perform combustion tests with two types of burners where each of the burners uses a different method to suppress NO<sub>x</sub> formation: (1) a fuel stage burner, (2) a fuel stage burner with internal flue gas recirculation. Each burner has different properties when using combustion air: (a) with ambient temperature and (b) with preheated air. The effect of the NO<sub>x</sub> reduction method and the effect of the combustion air temperature on the combustion parameters will be investigated and evaluated. The observed parameters will include NO<sub>x</sub> and CO emissions, the temperature distribution in the horizontal symmetry plane of the combustion chamber, heat transfer along the flame, colour and flame stability.

### **Master's Thesis goals:**

- 1) The Study of recommended data on process burner issues, their overview and assessment according to various criteria.
- 2) Working with research methods concerning preheating combustion air.

- 3) Combustion tests with a fuel stage burner.
- 4) Combustion tests with a fuel stage burner and integrated, internal flue gas recirculation.
- 5) An evaluation of experimental data.

**Recommended bibliography:**

BAUKAL, Charles E., ed. Industrial Burners Handbook. CRC Press, 2003. 808 s. ISBN 9780849313868.

BAUKAL, Charles E., ed. Industrial Combustion Pollution and Control. CRC Press, 2003. 916 s. ISBN 9780824746940.

BALLESTER, Javier M. et al. Investigation of low-NO<sub>x</sub> strategies for natural gas combustion. Fuel. 1997, 76 (5), 435-446. ISSN 0016-2361.

Students are required to submit the thesis within the deadlines stated in the schedule of the academic year 2018/19.

In Brno, 25. 10. 2018



prof. Ing. Petr Stehlík, CSc., dr. h. c.  
Director of the Institute

doc. Ing. Jaroslav Katolický, Ph.D.  
FME dean

## Abstract

This master's thesis deals with combustion air preheating and its influence on combustion process parameters. In the theoretical part, an overview of the most common air pollutants from industrial combustion is presented. The relevant currently valid legislation in the European Union is described and its implementations into national legislations in the Czech Republic and in Germany are compared. Furthermore, classification of burner types according to different criteria and a research on previous work concerning combustion air preheating are included. An experimental investigation of two different fuel-staged burners fired by natural gas at a constant thermal input of 750 kW with combustion air preheated up to 250 °C was carried out at a burner testing facility. The results revealed a positive effect of preheating on the combustion efficiency. On the contrary, the amount of produced emissions NO<sub>x</sub> and CO emissions increased with the preheating temperature.

## Keywords

Combustion air preheating, burner, heat flux, temperature distribution, emissions, nitrogen oxides

## Abstrakt

Tato diplomová práce se zabývá předehřevem spalovacího vzduchu a jeho vlivem na parametry spalovacího procesu. V teoretické části je zpracován přehled nejčastějších znečišťujících látek z průmyslového spalování. Je popsána aktuálně platná relevantní legislativa v Evropské unii a jsou porovnány její implementace do národní legislativy v České republice a v Německu. Dále je provedena klasifikace hořáků z hlediska různých kritérií a rešerše předchozí práce v oblasti předehřevu spalovacího vzduchu. Na zkušební hořáků byla provedena experimentální studie dvou různých hořáků na zemní plyn při konstantním tepelném příkonu 750 kW se spalovacím vzduchem předehřátým až na 250 °C. Výsledky odhalily pozitivní vliv předehřevu na účinnost spalování. Množství emisí NO<sub>x</sub> a CO naopak rostlo s teplotou spalovacího vzduchu.

## Klíčová slova

Předehřev spalovacího vzduchu, hořák, tepelný tok, rozložení teplot, emise, oxidy dusíku

## **Bibliographic citation**

ŠIMEČEK, Radek. *The influence of the combustion air temperature on parameters of the combustion process*. Brno: Vysoké učení technické v Brně, Fakulta strojního inženýrství, 2019. 70 p. Supervisor of the master's thesis: Ing. Pavel Skryja, Ph.D.

## Affirmation

I declare that this master's thesis is a result of my own work led by Ing. Pavel Skryja, Ph.D. and that I have not used any other sources of information than listed in references.

Brno, 24<sup>th</sup> of May 2019

.....

Bc. Radek Šimeček

## **Acknowledgments**

Hereby I would like to express my sincere gratitude to the supervisor of this thesis Ing. Pavel Skryja, Ph.D. for providing valuable advices, to Ing. Petr Bělohradský, Ph.D. for his assist with carrying out the experimental part, and to Prof. Dr.-Ing. Marcus Reppich for helping me during my studies at Hochschule Augsburg. Last but not least, I would like to thank my family for supporting me during my entire studies.

# Contents

<b>1</b>	<b>Introduction .....</b>	<b>10</b>
1.1	Aims of the thesis.....	11
<b>2</b>	<b>Combustion pollutants .....</b>	<b>12</b>
2.1	Nitrogen oxides.....	12
2.2	Sulphur oxides .....	13
2.3	Carbon dioxide.....	14
2.4	Carbon monoxide.....	15
<b>3</b>	<b>Legislation .....</b>	<b>16</b>
3.1	European Union .....	16
3.1.1	European Pollutant Release and Transfer Register .....	17
3.2	Czech Republic .....	17
3.2.1	Integrated pollution register.....	20
3.3	Germany.....	21
3.3.1	Thru.de.....	23
<b>4</b>	<b>Heat transfer .....</b>	<b>25</b>
4.1	Conduction.....	25
4.2	Convection .....	25
4.3	Radiation .....	26
<b>5</b>	<b>Types and classification of burners.....</b>	<b>27</b>
5.1	Mixing type.....	27
5.1.1	Diffusion burners .....	27
5.1.2	Premixed burners .....	27
5.2	Fuel type.....	28
5.2.1	Gaseous fuel .....	28
5.2.2	Liquid fuel .....	28
5.2.3	Solid fuel.....	28
5.3	Oxidizer type.....	28
5.3.1	Atmospheric air combustion.....	28
5.3.2	Oxygen-enhanced combustion .....	29
5.4	Draft type .....	30
5.4.1	Natural draft.....	30
5.4.2	Forced draft.....	30
<b>6</b>	<b>Combustion air preheating .....</b>	<b>31</b>
6.1	Devices for preheating .....	33
6.1.1	Recuperators .....	33



---

6.1.2	Regenerators .....	33
6.2	Previous research .....	34
<b>7</b>	<b>Experimental investigation .....</b>	<b>37</b>
7.1	Burner testing facility .....	37
7.1.1	Combustion chamber .....	38
7.1.2	Combustion air preheater.....	38
7.1.3	Measurement instrumentation .....	39
7.2	Burners.....	40
7.2.1	Fuel-staged burner .....	40
7.2.2	Fuel-staged burner with internal recirculation.....	42
7.3	Experimental setup.....	42
<b>8</b>	<b>Results.....</b>	<b>44</b>
8.1	NO <sub>x</sub> emissions.....	44
8.2	CO emissions .....	45
8.3	Flue gas temperature .....	46
8.4	Heat fluxes .....	47
8.5	Efficiency of the radiant section .....	50
8.6	Temperature distribution.....	52
8.7	Flame stability.....	57
8.8	Flame pattern .....	59
<b>9</b>	<b>Conclusions.....</b>	<b>60</b>
	<b>List of symbols .....</b>	<b>62</b>
	<b>List of chemical formulas.....</b>	<b>63</b>
	<b>List of abbreviations.....</b>	<b>63</b>
	<b>List of figures .....</b>	<b>64</b>
	<b>List of tables .....</b>	<b>66</b>
	<b>References.....</b>	<b>66</b>

# 1 Introduction

Industrial combustion is a complex topic, which has been widely discussed in recent times since heat is an essential requirement in the process industry. Most of the industrial heating processes are characterized by demand on large amount of energy. Nowadays, the major energy source for heat and power generation is burning of fossil fuels. According to the data provided by the International Energy Agency, the contribution of fossil fuels (coal, oil and natural gas) to the total primary energy supply <sup>1</sup> worldwide has not changed significantly in the past decades (86 % in 1971; 81 % in 2016) [1]. However, the global primary energy supply is increasing on a long-term basis, as shown in Fig. 1, which leads to an increase in the amount of pollutant emissions produced by combustion of fuels. These pollutants (e.g. nitrogen and sulphur oxides, carbon monoxide and dioxide, volatile organic compounds and particulate matter) have a negative impact on human health as well as on the environment in general.

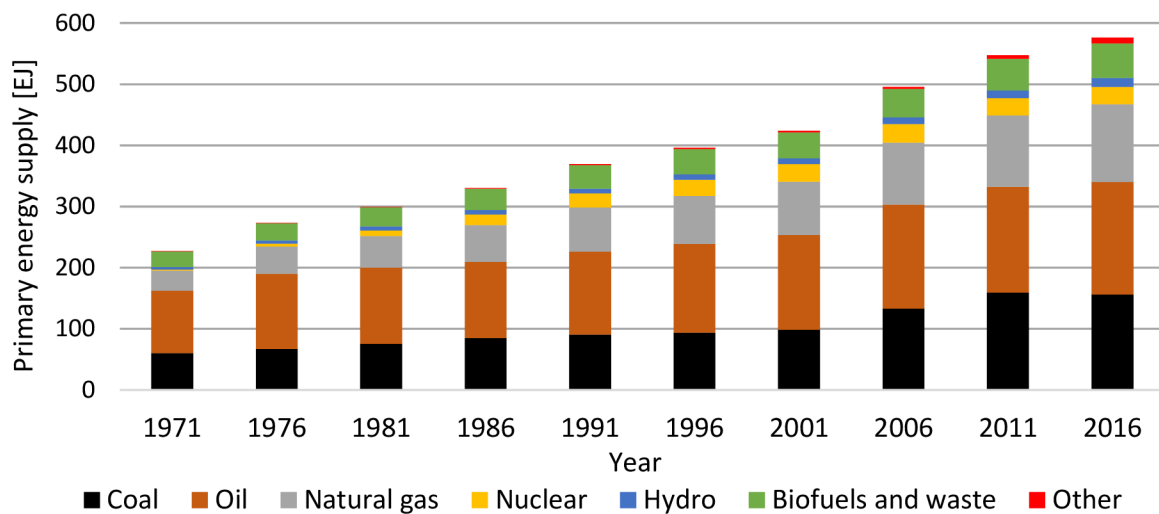


Fig. 1: Primary energy supply worldwide in exajoules between 1971 and 2016; data from [1]

In recent years, some developed countries have announced their plans to significantly reduce the use of certain fossil fuels for energy production and to replace them by low-carbon or renewable sources of energy in order to reduce pollutant emissions into air. For example, the government of United Kingdom decided in November 2015 that all coal-fired power stations will be restricted from their usage from 2023 and must close by 2025 at latest. These coal power plants should be replaced with a new generation of gas-fired power plants [2]. Coal-fired power plants in Germany should be shut down by 2038 at latest, as decided by a government-appointed commission in January 2019 [3]. Concurrently, Germany will retreat from using nuclear energy by 2022 and will thus become the first developed industrialized country in the world which phases out both coal and nuclear energy at the same time [4]. However, combustion of fuels in general will most likely remain irreplaceable in process industry and power generation even in the future.

Operating a combustion process requires consideration of multiple factors. In order to minimize the operating costs, waste heat from the process is utilized in most industrial applications. A common possibility is to reuse the waste heat energy for preheating the supplied combustion air. This can be an effective tool for saving fuel and reducing costs. Moreover, combustion air preheating may be useful in a wide variety of industrial applications

<sup>1</sup> Primary energy is any energy commodity that can be captured directly from natural resources [1]

which require high temperatures, for example metal processing or glass production. Another priority with respect to relevant environmental regulations is minimizing the amount of produced pollutant emissions. Any change in combustion air temperature may however affect parameters of the overall combustion process. A negative consequence of combustion air preheating may be an increase in amount of NO<sub>x</sub> and CO emissions [5]. Thus, it is an important engineering task to design the process and to find the optimal operating conditions, taking these factors into consideration.

## 1.1 Aims of the thesis

In the first chapter of this master's thesis, an overview of the most common pollutants from industrial combustion will be presented, including their formation mechanisms and abatement strategies. Further, the currently valid legislation in the European Union concerning emissions from industrial combustion will be described with focus on its transpositions into national legislations in the Czech Republic and in Germany. Moreover, data from national pollution release and transfer registers on NO<sub>x</sub> production in these countries will be presented. Another chapter will deal with the basic mechanisms of heat transfer, followed by a classification of burner types according to different criteria (draft, fuel, oxidizer and mixing type). The previous research work on combustion air preheating will be summed up.

An experimental investigation will be carried out at a large-scale burner testing facility at Faculty of Mechanical Engineering in Brno, which is equipped with a combustion air preheater. In contrast to most industrial applications, an auxiliary natural gas burner will be used for preheating instead of waste heat in order to ensure a precise control of the combustion air temperature. The tests will be performed with two different natural gas burners: a fuel-staged burner and a fuel-staged burner with integrated flue gas recirculation.

The aim of this investigation is to reveal the impact of combustion air preheating on the combustion process parameters. Among the most important parameters are NO<sub>x</sub> and CO emissions, flue gas temperature and heat fluxes to the water-cooled shell of the combustion chamber. Based on the heat fluxes and total heat input to the chamber, efficiency of the radiant section will be calculated according to API standards. In addition to this, temperatures inside the chamber will be measured and the resulting temperature profiles will be visualised. The stability of combustion as well as flame colour and length will be observed even at different oxygen concentrations in the flue gas. All these parameters will be investigated for combustion air temperatures ranging from 20 °C to 250 °C. Finally, the obtained experimental data will be evaluated and discussed.

## 2 Combustion pollutants

### 2.1 Nitrogen oxides

Most of the world's nitrogen occurs naturally as inert gas contained in the atmospheric air, which consists of approximately 78%  $N_2$  by volume [6]. There are generally seven oxides of nitrogen, however, only nitrogen monoxide (NO, known also as nitric oxide) and nitrogen dioxide ( $NO_2$ ) are relevant with respect to emissions from combustion processes. These two oxides are together commonly referred as  $NO_x$ .

Nitrogen monoxide is a colourless gas, which is poisonous to humans and can cause for example irritation of the eyes and throat, nausea or headache. Nitrogen monoxide is the predominant  $NO_x$  compound formed in combustion processes and a precursor to the formation of  $NO_2$  in the atmosphere. Nitrogen dioxide, a reddish-brown gas, is a strong oxidizing agent. It is highly toxic and hazardous because of its ability to enter into the bloodstream, causing disruption of oxygen supply similarly to carbon monoxide [7]. Moreover, nitrogen oxides decompose in the presence of sunlight into ozone and are thus responsible for ground-level ozone formation. Together with sulphur oxides contribute the  $NO_x$  to the formation of acid rain as they react with moisture present in the atmosphere to form nitric acid ( $HNO_3$ ) [6].

There are three generally accepted mechanisms for  $NO_x$  formation. The first type of  $NO_x$  with respect to the formation mechanism is referred as *thermal* or *Zeldovich*  $NO_x$ . It is produced as a result of a reaction between oxygen and nitrogen in the oxidizer at high temperatures. The amount of produced thermal  $NO_x$  emissions increases exponentially with temperature. It is the predominant mechanism in combustion processes over 1100 °C. Generally, it is possible to reduce the emissions of thermal  $NO_x$  by reducing the reaction time, temperature, and overall concentrations of  $N_2$  and  $O_2$  in the combustion system [8].

Another formation mechanism, known as *prompt* or *Fenimore*  $NO_x$ , occurs as a result of a relatively fast reaction between nitrogen, oxygen and hydrocarbon radicals [6]. It is actually a complex process consisting of hundreds of reactions with hydrogen cyanide (HCN) as an intermediate product. Increasingly important becomes the prompt mechanism under very rich fuel conditions. However, these are not very common in the most combustion processes and this mechanism is thus less significant compared to the two other formation mechanisms [8].

The third mechanism of  $NO_x$  formation is the so-called *fuel* or *de Soete* mechanism. It is the dominant mechanism during combustion of fuels which contain higher amount of organically bound nitrogen, e.g. coal or heating oils. For these fuels, the contribution of the fuel  $NO_x$  to the total  $NO_x$  may range 50 to 95 % [8]. The reason is that the N–H and N–C bonds, common in fuel-bound nitrogen, are weaker than the triple bond  $N\equiv N$  in molecular nitrogen, which must be dissociated to produce thermal  $NO_x$ . In contrast to this, the amount of produced fuel  $NO_x$  is negligible for most gaseous fuels like natural gas due to a very small amount of bound nitrogen [6].

The measures for  $NO_x$  control can be divided into two basic categories. The primary measures include combustion modifications where the  $NO_x$  production is reduced directly during the combustion process. As an example may serve staged supply of oxidizer or fuel, flue gas recirculation, or injection of water steam into the combustion chamber. The aim of the secondary (or post-combustion) methods is to reduce the already formed nitrogen oxides. The most common secondary methods are selective catalytic or non-catalytic reduction, using ammonia or urea as reduction agent [9]. The methods for  $NO_x$  reduction as well as the formation mechanisms were already described more in detail in previous work [10].

## 2.2 Sulphur oxides

With respect to emissions from combustion processes, the sulphur oxides referred as  $SO_x$  include sulphur dioxide ( $SO_2$ ) and sulphur trioxide ( $SO_3$ ). Sulphur dioxide is a colourless acidic gas with a pungent odour, which can be registered by human olfactory sense at concentrations over 3 ppm. Concentrations of  $SO_2$  higher than 10 ppm irritate the upper respiratory tract and may cause among other things breathing problems by reaction with moisture in the respiratory system [7]. In the atmosphere, sulphur oxides react with water to form sulphurous and sulfuric acid (equations (2.1) and (2.2)), which are in diluted form components of acid rain [6]:



Thus, the sulphur oxides are generally responsible for accelerating metal corrosion. Sulphur dioxide is according to Miller [8] the most detrimental pollutant that contributes to metals corrosion. Higher temperatures and relative humidity significantly influence the rate of corrosion. Sulphurous and sulphuric acids are also capable of damaging a wide variety of building materials including e.g. limestone or marble [6].

All fossil fuels contain a certain amount of sulphur or sulphur compounds. Fuels like heavy heating oil and coal generally contain significant amounts of sulphur, while gaseous fuels like natural gas tend to contain little or no sulphur. Since the oxidizer typically does not contain any sulphur, is the fuel the only source of sulphur for  $SO_x$  formation. This is a difference in comparison to the nitrogen oxides (chapter 2.1), which can be formed from nitrogen contained both in fuel and oxidizer. The amount of  $SO_x$  emissions from combustion cannot be thus affected by any changes of the burner setting.

The formation process of sulphur oxides may be described in two steps. In the first oxidation step, the sulphur is in high-temperature combustion processes oxidized by oxygen from the combustion air to form  $SO_2$ , according to the overall reaction (2.3) [6]:



The second step of sulphur oxidation is described by the following equation (2.4):



The formation of sulphur dioxide occurs predominantly at higher temperatures, while sulphur trioxide is more preferred at lower temperatures. Typically, due to high temperatures in the most combustion systems is the ratio of  $SO_2$  to  $SO_3$  on the order of 40–80:1. The second step is than more probable to occur in the atmosphere after leaving the combustor, since the equilibrium strongly favours formation of  $SO_3$  at ambient temperatures [6].

There are several basic abatement strategies of  $SO_x$ . The first strategy involves pre-treating the incoming fuel, oxidizer, or feed materials, which leads to reducing overall sulphur content at input into the combustion system. This is usually referred as (fuel) desulfurization. Examples of this can be cleaning coal in order to remove components such as pyrite [8], or replacing the fuel with another one which contains less sulphur. However, switching to another fuel may be uneconomical in some cases [6].

Another possibility to reduce  $SO_x$  emissions is based on modifications of the combustion process. An alternative to burning coal in traditional combustors is to use a fluidized bed combustor where the bed contains e.g. limestone particles. The limestone reacts with the

sulphur oxides to form  $\text{CaSO}_4$ , which can be subsequently scrubbed out in the exhaust gas treatment system [6].

The third strategy is focused on post-combustion treatment of the flue gases. Generally, the systems for flue gas desulphurization (FGD) can be classified as wet scrubbers or dry scrubbers. A wet FGD process produces a slurry waste, while a dry FGD application results in solid waste, which makes the transport and disposal easier compared to the waste from wet FGD [8].

## 2.3 Carbon dioxide

Carbon dioxide ( $\text{CO}_2$ ) is a colourless, odourless and inert gas that does not support life since it can displace oxygen and act as an asphyxiant. It is found naturally in the atmosphere at concentrations averaging 300 ppmv. Concentrations of 6 to 10 % vol. can cause headaches and visual disturbances. At concentrations above 10 %, unconsciousness eventually leading to death may occur [6].

As a significant greenhouse gas, carbon dioxide absorbs and emits radiation from the atmosphere within the thermal infrared range, which results in an increase in the average surface air temperature of the planet, referred as global warming [7]. The concentration of  $\text{CO}_2$  in the Earth's atmosphere is increasing on a long-term basis, as it is obvious from the so-called Keeling curve (Fig. 2). This curve depicts the  $\text{CO}_2$  concentrations in the atmosphere, measured since 1958 on the island of Hawaii. The location was chosen in order to avoid any influences of urban pollution on the measurements. Characteristic for the Keeling curve are the regular fluctuations of the  $\text{CO}_2$  level during a year cycle, corresponding to the seasonal vegetation changes [11].

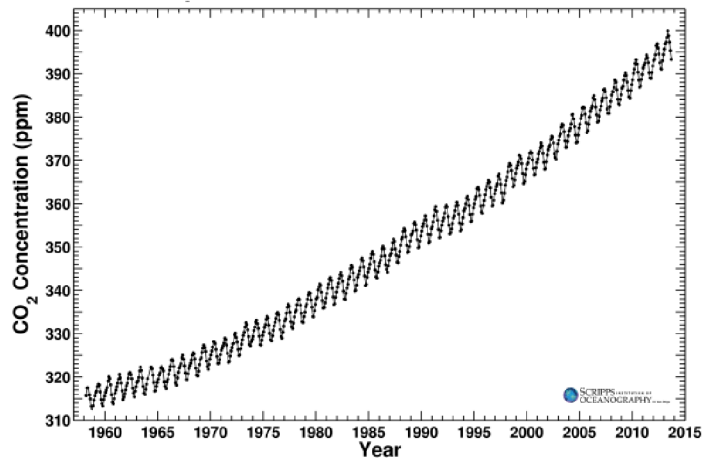


Fig. 2: Average monthly  $\text{CO}_2$  concentrations in the atmosphere, depicted by the Keeling curve [11]

Carbon dioxide is a naturally occurring part of the natural cycle in the atmosphere, which is removed by photosynthesis. However, the major source of  $\text{CO}_2$  released into the atmosphere is combustion of carbon-containing fuels near or above the stoichiometric conditions. Since emissions of carbon dioxide are unavoidable during combustion of fossil fuels, most of the abatement and control strategies for  $\text{CO}_2$  involve improving the overall thermal efficiency of the combustion system so that less fuel needs to be consumed for a given level of production. Another possibility is to sequester the resulting  $\text{CO}_2$  in some form so that it does not contribute to the growing increase in its concentration in the atmosphere [6]. The recent trends in this field include for example development of new adsorbents for post-combustion  $\text{CO}_2$  capture [12].

## 2.4 Carbon monoxide

Carbon monoxide (CO) is a colourless, odourless and tasteless flammable gas. Nevertheless, it is a highly poisonous compound due to its much greater affinity for haemoglobin (approximately 300 times [6]) compared to oxygen. When inhaled, carbon monoxide enters the bloodstream and disrupts the supply of oxygen to the body's tissues, which may result to death at concentration of ca. 1000 ppm or higher [7]. Even at low concentrations, CO may have negative influence on mental function, vision, and alertness of the affected person [6].

Generally, carbon monoxide is produced during incomplete combustion of carbon-containing fuels. This occurs if there is an insufficient amount of oxygen for a complete combustion, or the temperature is not high enough to oxidize the fuel completely, or the residence time in the combustion zone is insufficient. The amount of CO emissions is therefore an important parameter, which indicates the completeness of combustion. Commonly, industrial combustion systems are operated under slightly lean conditions (with O<sub>2</sub> excess) to ensure a complete combustion and to minimize the CO emissions [5].

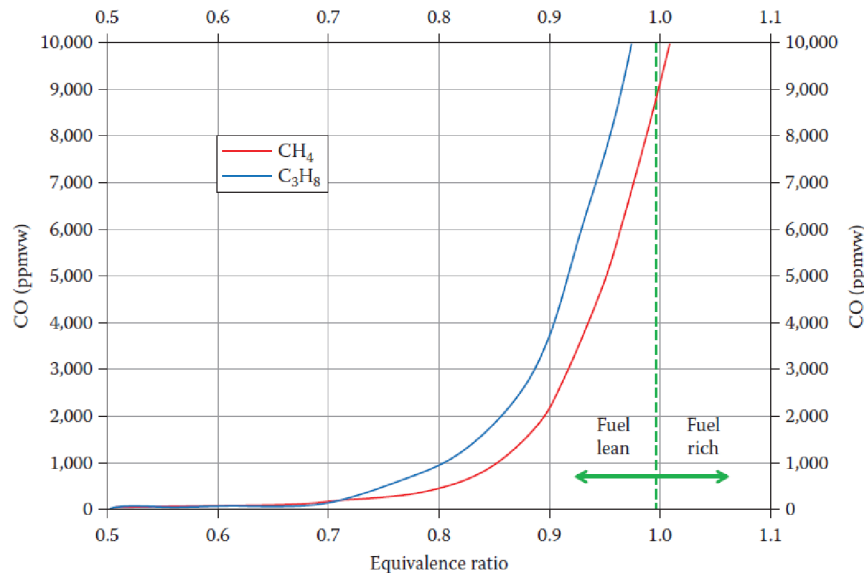


Fig. 3: Carbon monoxide emissions as a function of equivalence ratio for two different fuels [5]

As can be seen in Fig. 3, it is obvious that the amount of produced CO emissions is strongly dependent on the equivalence ratio<sup>2</sup>. With decreasing combustion air surplus, CO emissions increase rapidly. At fuel rich conditions, the CO concentration is even higher than 10 000 ppm for the both considered fuels.

The abatement strategies are primarily based on catalytic oxidation of CO to CO<sub>2</sub>. This is typically done at temperatures between 400 and 500 °C. The higher is the temperature, the higher is the destruction efficiency. If the temperature is high enough, then no catalyst is needed. The catalyst is only needed when it would be more expensive to heat the flue gases up to a sufficient temperature [5]. The catalyst can be based for example on manganese oxides, as proposed by Mobini et al. [13]. Without any catalytic oxidation, the lifetime of carbon monoxide in the atmosphere is fairly long, on the order of two to four months, before it is oxidized to carbon dioxide [5]. Consequently, CO may be also indirectly considered as a greenhouse gas due to formation of CO<sub>2</sub> as its oxidation product.

<sup>2</sup> Equivalence ratio  $\Phi$  is defined as the actual fuel-air ratio divided by the stoichiometric fuel-air ratio.

## 3 Legislation

### 3.1 European Union

Since the 1970s, the European Union has developed a complex legal framework for tackling air pollution [14]. The member countries are responsible for implementing the European directives into their national legislations. Currently, the basic legislative sources concerning emissions from industrial combustion in the EU are the following directives of the European Parliament and of the Council:

- 2001/81/EC on national emission ceilings for certain atmospheric pollutants
- 2008/50/EC on ambient air quality and cleaner air for Europe
- 2010/75/EU on industrial emissions (integrated pollution prevention and control)
- 2015/2193 on the limitation of emissions of certain pollutants into the air from medium combustion plants
- 2016/2284 on the reduction of national emissions of certain atmospheric pollutants

The directive 2001/81/EC was adopted in 2001 to set national ceilings of the major air pollutants emissions in order to improve the protection of the environment and human health against effects of acidification, soil eutrophication and ground-level ozone. Another aim was to move towards the long-term objectives of not exceeding critical levels of pollution, taking the years 2010 and 2020 as benchmarks [15]. Currently (2019), the directive 2001/81/EC is no longer in force, except for Articles 1 to 4 which are valid until the 31<sup>st</sup> of December 2019. In 2016, this directive was revised and newly entered in force as directive no. 2016/2284, which is setting out national emission reduction commitments of each member country for year 2030 in compliance with the revised Gothenburg Protocol<sup>3</sup>.

In chapter II of the directive 2008/50/EC, requirements on member countries regarding assessment of ambient air quality are specified. Pursuant to Article 4 shall the member countries establish zones and agglomerations throughout their territories in order to assess the air quality. Further, the criteria for locations of sampling points for the pollutant measurements are listed in Annex III to this directive.

In the directive 2015/2193, emission limits for combustion plants with a rated thermal input equal to or greater than 1 MW and less than 50 MW (referred as medium combustion plants) are specified. The values of these limits for SO<sub>2</sub>, NO<sub>x</sub> and dust are stated in Annex III separately for new and existing plants.

The directive no. 2010/75/EU was designed in order to control, prevent and reduce emissions of NO<sub>x</sub>, CO and SO<sub>2</sub> into air, water and soil from specific sources of pollution listed in Annex I to this directive. Technical provisions relating to combustion plants with total rated thermal input equal to or greater than 50 MW are stated in Annex V. With respect to the emission limits, the installations are divided into two groups. The installations, which have been granted a permit before 7<sup>th</sup> January 2013, or a complete application for a permit has been submitted before that date and the installation was put into operation no later than 7<sup>th</sup> January 2014, shall not exceed the emission limits set out in Part 1 of Annex V. For the other installations, the limit values are stricter and are stated in Part 2 *ibid*. On these limit values are based the national legislations in the EU member countries.

---

<sup>3</sup> Gothenburg Protocol to abate acidification, eutrophication and ground-level ozone



In the directive 2016/2284, long-term objectives of achieving air quality levels are set out. The national emission reduction commitments for reduction of NO<sub>x</sub>, SO<sub>2</sub>, ammonia, non-methane volatile organic compounds and fine particulate matter are established. For this purpose, national air pollution control programmes are required to be drawn up, adopted and implemented. The commitments are applicable from 2020 to 2029 and from 2030 onwards, as laid down in Annex II to this directive. The emission reduction targets for particular member countries are expressed in this Annex as percentual change in comparison to emissions produced in the year 2005.

In the following chapters 3.2 and 3.3 of this thesis, the transposition of the above mentioned directives into national legislation is described for the Czech Republic and for Germany. Moreover, valid emission limits of nitrogen oxides and carbon monoxide are stated, since these emissions can be affected by changing the burner setting. Besides that, the amount of CO emissions is an important parameter giving information about the completeness of the combustion process.

### **3.1.1 European Pollutant Release and Transfer Register**

The European Pollutant Release and Transfer Register (E-PRTR) provides since 2006 data concerning pollutant releases to air, water and soil, as well as information about waste transfers from installations covered by Annex I of the regulation 166/2006/EC. It is built on the same principles as the previous European Pollutant Emission Register (EPER) but includes reporting of more pollutants and activities. The 91 currently monitored pollutants are listed in Annex II to this regulation along with the threshold values, over which the releases must be reported. The E-PRTR is administrated by the European Environment Agency (EEA).

The term installation is in 166/2006/EC defined in Article 2 as '*a stationary technical unit where one or more activities listed in Annex I are carried out, and any other directly associated activities which (...) could have an effect on emissions and pollution*' [16].

The aim of E-PRTR is to provide public access to information on releases of pollutants. Concurrently, it is a cost-effective tool for encouraging improvements in environmental performance, for tracking trends and demonstrating progress in pollution reduction [15].

These objectives can only be achieved if the data reported by the EU member states are reliable and comparable. An adequate harmonisation of the data collection is therefore needed to ensure the quality and comparability of data. Pursuant to Article 7 of 166/2006/EC, the member states shall provide the required data within 15 months after the end of the reporting year, where the first reporting year was 2007. Subsequently, the European Environment Agency incorporates the information reported by the member states into the E-PRTR [15]. Moreover, the member countries gather the data about pollutants emissions in their own national PRTRs (see chapters 3.2.1 and 3.3.1).

## **3.2 Czech Republic**

In the Czech Republic, the key legislative document concerning to emissions from industrial combustion is the Act no. 201/2012 Sb. on the protection of air<sup>4</sup>, which entered into force on 1<sup>st</sup> September 2012 and replaced the previous Act no. 86/2002 Sb.<sup>5</sup>

A stationary source of pollution is defined in § 2 as '*compact, technically indivisible unit or activity, which pollutes or could pollute and is not used exclusively for research, development*

---

<sup>4</sup> Zákon č. 201/2012 Sb., o ochraně ovzduší

<sup>5</sup> Zákon č. 86/2002 Sb., o ochraně ovzduší

or testing purposes'. A combustion stationary source means in terms of this Act 'a stationary source, in which fuels are oxidized in order to utilize the released heat'.

Annex 1 to the Act 201/2012 Sb. contains a list of activities with accordance to the directive 2010/75/EU. Moreover, for each activity it is stated, if a dispersion study, compensation measures or operating rules pursuant to § 11 of this Act are required. The emission limits are divided into two types: general and specific. The general limits for polluting substances can be used only in case that no specific limits are defined in the operating permit for the particular installations.

The specific emission limits for stationary sources of pollution with rated thermal input lower than or equal to 300 kW are stated in Annex 10, Part II to the Act no. 201/2012 Sb., related to standard conditions<sup>6</sup> and reference oxygen content 3 % in dry flue gas. The limit values of NO<sub>x</sub> and CO are presented in Tab. 1. For solid fuels, limits of NO<sub>x</sub> are not given.

Tab. 1: Specific emission limits [mg·m<sup>-3</sup>] for stationary sources with rated thermal input lower than or equal to 300 kW valid in the Czech Republic from 1.1.2018 [17]

Fuel	NO <sub>x</sub>	CO
Liquid	130	80
Gaseous	65	80

In comparison to the limits valid up to 31<sup>st</sup> December 2017, the currently valid limits of NO<sub>x</sub> are for gaseous fuels tightened from 120 to 65 mg·m<sup>-3</sup>, limits of CO are tightened for both types of fuel from 100 to 80 mg·m<sup>-3</sup>.

Another important legislative document on emission limits is Regulation no. 415/2012 Sb. on the permitted level of pollution and its ascertainment<sup>7</sup>, which processes the relevant directives of the EU. Above all, general and specific emission limits for operation of stationary sources of pollution and methods of evaluation of their fulfilment are given by this regulation. Furthermore, methods for ascertainment of the level of pollution and general provisions to combustion of fuels are described. As given in Annex 9, the general emission limit of nitrogen oxides expressed as nitrogen dioxide is 500 mg·m<sup>-3</sup> for mass flow rates higher than 10 kg·h<sup>-1</sup>. The mass concentration of carbon monoxide shall not exceed 500 mg·m<sup>-3</sup> for mass flow rates higher than 5 kg·h<sup>-1</sup>, related to standard conditions.

In Part II of Annex II to the regulation 415/2012 Sb. are stated the specific emission limits for stationary combustion sources of pollution with rated thermal input greater than 0.3 MW and lower than 50 MW. For this purpose, the sources of pollution are divided into three groups. In the first group, piston combustion engines are included. The second group is comprised of boilers and hot air direct heating stationary sources, while the last group contains gas turbines. These limits, presented in Tab. 2, are related to normal conditions and dry gas. The reference oxygen content is 6 % for solid fuels excluding biomass, 11 % for biomass and 3 % for gaseous and liquid fuels. Moreover, limit values valid from 1<sup>st</sup> January 2025 are further stated, the limits of NO<sub>x</sub> and CO will however remain unaffected for sources of pollution put into

<sup>6</sup> The standard conditions are defined as a temperature of 273.15 K and an absolute pressure of 101.325 kPa.

<sup>7</sup> Vyhláška č. 415/2012 Sb., o přípustné úrovni znečišťování a jejím zjišťování a o provedení některých dalších ustanovení zákona o ochraně ovzduší

operation on 20<sup>th</sup> December 2018 and later. For the sources put into operation before this date, new exceptions concerning certain types of fuels are added.

Tab. 2: Specific emission limits [ $\text{mg}\cdot\text{m}^{-3}$ ] valid in the Czech Republic from 20.12.2018 up to 31.12.2024 for stationary sources with rated thermal input greater than 0.3 MW and lower than 50 MW, excluding piston combustion engines and gas turbines [18]

Fuel	> 0.3 – 1 MW		> 1 – 5 MW		> 5 – 50 MW	
	NO <sub>x</sub>	CO	NO <sub>x</sub>	CO	NO <sub>x</sub>	CO
Solid fuel excluding biomass	600	400	500	500	500	300
Biomass			333		200	500 <sup>a)</sup>
Liquid fuels	200	80	200	80	200	80
Gaseous fuels	100 <sup>b)</sup>	50	100 <sup>b)</sup>	50	100 <sup>b)</sup>	50

Notes: a) 300  $\text{mg}\cdot\text{m}^{-3}$  for biomass pressings; b) 200  $\text{mg}\cdot\text{m}^{-3}$  if not possible to meet the limit 100  $\text{mg}\cdot\text{m}^{-3}$  by using low-emission burners

The Part I of Annex II to 415/2012 Sb. contains values of specific emission limits for combustion stationary sources with a total rated heat input power of 50 MW and greater. In accordance with 2010/75/EU, these installations are divided into two groups: the first group comprises installations, for which a complete application for a permit has been submitted before 7<sup>th</sup> January 2013 and the installation was put into operation no later than 7<sup>th</sup> January 2014. In the other group are those installations, which do not comply with these requirements. The limits for the other group of installations are presented in Tab. 3. Limit values of NO<sub>x</sub> are for certain fuels stricter by 50  $\text{mg}\cdot\text{m}^{-3}$  compared to the first group. The reference O<sub>2</sub> content is equal to 6 % for solid fuels and to 3 % for liquid and gaseous fuels.

Tab. 3: Specific emission limits [ $\text{mg}\cdot\text{m}^{-3}$ ] valid in the Czech Republic for stationary sources with rated thermal input 50 MW or greater, for which a complete application for a permit has been submitted on 7.1.2013 or later, or were put into operation after 7.1.2014 [18]

Fuel	50 – 100 MW		> 100 – 300 MW		> 300 MW	
	NO <sub>x</sub>	CO	NO <sub>x</sub>	CO	NO <sub>x</sub>	CO
Biomass and peat	250	250	200	250	150	250
Other solid fuels	300 <sup>a)</sup>	250	200	250	150 <sup>b)</sup>	250
Liquefied natural gas	300	175	150	175	150	175
Other liquid fuels	300	175	150	175	100	175
Gaseous fuels	100	100	100	100	100	100

Notes: a) 400  $\text{mg}\cdot\text{m}^{-3}$  for pulverized brown coal; b) 200  $\text{mg}\cdot\text{m}^{-3}$  in fluidized bed

More in detail are the legislative regulations and measures regarding emissions from industrial combustion in the Czech Republic, including emission ceilings and national emission projection, described for example in [10].

### 3.2.1 Integrated pollution register

A publicly accessible database of transfers of selected substances into the environment in accordance with the European directive regulation 166/2006/EC is in the Czech Republic known as Integrated pollution register (IRZ)<sup>8</sup>. It is run by Czech Environmental Information Agency (CENIA)<sup>9</sup>, a state-funded organisation of Ministry of the Environment<sup>10</sup>. Currently, releases and transfers of 93 substances are monitored [19]. The list of these substances as well as thresholds for their reporting are part of Act no. 25/2008 Sb.<sup>11</sup>, which is the key document for establishing this national pollutant release and transfer register. In the year 2017, pollutant transfers and releases from total 1338 facilities were reported. In the Tab. 4 below are presented the top five producers of NO<sub>x</sub> emissions in the Czech Republic,

Tab. 4: The top five NO<sub>x</sub> emissions producers in the Czech Republic, 2017 [20]

No.	Facility	Main activity	Region	NO <sub>x</sub> [t/y]
1.	Elektrárna Počerady, a.s.	Thermal power station	Ústecký	5 518
2.	ČEZ, a.s., Elektrárny Pruněřov	Thermal power station	Ústecký	3 866
3.	ČEZ, a.s., Elektrárna Mělník	Thermal power station	Středočeský	3 133
4.	UNIPETROL RPA, s.r.o., Litvínov	Chemicals production	Ústecký	3 199
5.	Sev.en EC, a.s., Elektrárna Chvaletice	Thermal power station	Pardubický	2 867

The Fig. 4. shows average yearly concentrations of nitrogen oxides reported by Czech Hydrometeorological Institute (ČHMÚ)<sup>12</sup>. It proves that the most significant sectors with respect to production of nitrogen oxides are industry and transport. The highest concentrations of NO<sub>x</sub> were measured in large cities (Praha, Brno), in industrial regions (Ústecký region, Ostravsko–Karvinsko) and near the most frequented roads. This is in correlation with the data presented in Tab. 4, since three out of top five NO<sub>x</sub> producers in the Czech Republic are located in the northern part of the country in Ústecký region.

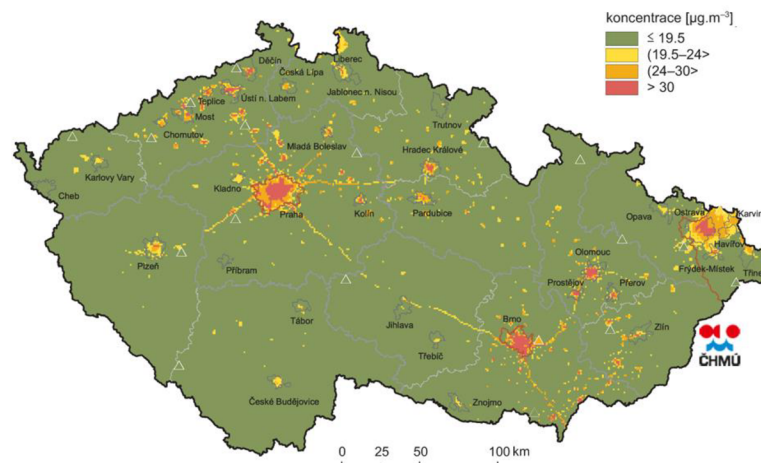


Fig. 4: Average yearly concentration of NO<sub>x</sub> in the Czech Republic, 2017 [21]

<sup>8</sup> Integrovaný registr znečišťování

<sup>9</sup> Česká informační agentura životního prostředí

<sup>10</sup> Ministerstvo životního prostředí

<sup>11</sup> Zákon č. 25/2008 Sb., o integrovaném registru znečišťování životního prostředí

<sup>12</sup> Český hydrometeorologický ústav

### 3.3 Germany

One of the basic legislative sources with respect to industrial combustion and emissions in the Federal Republic of Germany is the Federal Immission Control Act, also referred as *BImSchG*<sup>13</sup>. The purpose of this Act is to ensure integrated prevention and reduction of any harmful effects on the environment caused by emissions to air, water and soil in compliance with the directive 2010/75/EU. Its provisions shall apply to construction and operation of any stationary facilities, machines and other non-stationary technical facilities as well as vehicles [22].

The relevant terms are defined in § 3 of *BImSchG*. Harmful effects on the environment are defined as ‘any immissions which (...) are likely to cause any hazards, significant disadvantages or significant nuisances to the general public or the neighbourhood’, air pollution is pursuant to this act ‘any change in the natural composition of the air, especially through smoke, soot, dust, gases, aerosols, steam or odorous substances’. In the Part II of *BImSchG*, requirements for construction, licensing and operation of installations are stated. Part V contains general provisions on monitoring and improving air quality.

From the Federal Immission Control Act, altogether 44 Ordinances on the Implementation of the Federal Immission Control Act are derived. These are referred as *BImSchV*<sup>14</sup>. For the topic of industrial combustion, the most important ordinances are the following ones:

- 1<sup>st</sup> ordinance on small and medium-sized combustion plants
- 4<sup>th</sup> ordinance on installations requiring a permit
- 13<sup>th</sup> ordinance on large combustion plants and gas turbine plants
- 39<sup>th</sup> ordinance on air quality standards and emission ceilings

The 4<sup>th</sup> ordinance contains a list of different installation types requiring permit pursuant to Article 10 of the directive 2010/75/EU, similarly to the Act no. 201/2012 Sb. valid in the Czech Republic. For each type of installation, it is stated if a permitting procedure with participation of the public is required (pursuant to § 10 *BImSchG*) or a simplified permitting procedure without participating of the public can be carried out (§ 19 *BImSchG*).

The European directives 2001/81/EC and 2008/50/EC are directly implemented into the 39<sup>th</sup> ordinance, which i.e. defines tools for evaluating the air quality (Part 3) and states the values national emissions ceilings for SO<sub>2</sub>, NO<sub>x</sub>, NMVOC and NH<sub>3</sub> (Part 7).

The emission limits for installations with thermal input of 50 MW or greater are contained in the 13<sup>th</sup> ordinance. For this purpose, the fuels are divided into four groups: solid fuels (§ 4), biofuels (§ 5), liquid (§ 6) and gaseous fuels (§ 7). The reference content of O<sub>2</sub> in flue gas is equal to 3 % vol. for liquid and gaseous fuels and 6 % vol. for solid and biofuels. In the Tab. 5, the values of emission limits pursuant to the 13. *BImSchV* are presented.

Another important document with regard to air pollution control is called *Technical Instructions on Air Quality Control*, commonly referred as *TA Luft*<sup>15</sup>. These technical instructions serve to protect the general public and the neighbourhood against harmful effects of air pollution on the environment and to provide precautions against harmful effects of air pollution in order to attain a high level of protection for the environment altogether, taking the best available techniques into consideration [24]. The currently valid version of *TA Luft* entered into force in 2002. However, a proposal of a new version was issued in 2018 [25].

<sup>13</sup> Bundes-Immissionsschutzgesetz

<sup>14</sup> Verordnungen zur Durchführung des Bundes-Immissionsschutzgesetzes

<sup>15</sup> Technische Anleitung zur Reinhaltung der Luft

Tab. 5: Emission limits [ $\text{mg}\cdot\text{m}^{-3}$ ] for installations with thermal input greater than 50 MW valid in Germany [23]

Fuel	> 50 – 100 MW		> 100 – 300 MW		> 300 MW	
	NO <sub>x</sub>	CO	NO <sub>x</sub>	CO	NO <sub>x</sub>	CO
Brown coal	400	150	200	200	200	200
Other solid fuels	300		200		150	
Untreated wood	250	150	250	200	150	200
Other biofuels		250		250		250
Liquid fuels	300 <sup>a)</sup>	80	150	80	100	80
Natural gas	100	50	100	50	100	50
Other gaseous fuels	200 <sup>b)</sup>	80 <sup>c)</sup>	200 <sup>b)</sup>	80 <sup>c)</sup>		80 <sup>c)</sup>

Notes: a)  $250 \text{ mg}\cdot\text{m}^{-3}$  for light heating oils; b)  $100 \text{ mg}\cdot\text{m}^{-3}$  for use in refineries; c)  $100 \text{ mg}\cdot\text{m}^{-3}$  for blast furnace gas and coke gas

Pursuant to chapter 5.2 of the *TA Luft*, the nitrogen oxides belong to class IV of inorganic gaseous substances. Therefore, their content in waste gas indicated as NO<sub>2</sub> shall not exceed a mass concentration of  $350 \text{ mg}\cdot\text{m}^{-3}$  under standard conditions. In waste gas generated by thermal or catalytic post-combustion facilities, concentration of NO<sub>x</sub> emissions shall not exceed  $200 \text{ mg}\cdot\text{m}^{-3}$  and simultaneously, CO emissions shall not exceed  $100 \text{ mg}\cdot\text{m}^{-3}$ . At installations emitting gaseous substances in excess of given mass flow rates, concentrations of the respective substances shall be measured continuously. This threshold value is equal to  $30 \text{ kg}\cdot\text{h}^{-1}$  for nitrogen oxides.

Further, special requirements for certain types of installations are stated in the chapter 5.4 of the *TA Luft*, including limit values for emissions of i.e. total dust, inorganic particulate matter, nitrogen oxides, sulphur oxides, carbon monoxide and organic substances.

The emission limits valid for combustion installations for generating of electricity, steam, hot water, process heat or hot waste gas with a rated thermal input of less than 50 MW are shown in Tab. 6. The reference oxygen level in flue gas is 11 % for solid fuels and 3 % vol. for liquid and gaseous fuels. Compared to the emission limits valid in the Czech Republic, the installations in Germany are not further divided into more categories according to their thermal input in order to assign the limits.

In October 2018, the 44<sup>th</sup> ordinance on medium-sized combustion plants, gas turbine plants and combustion engines was approved by the German Bundestag as a direct implementation of the European directive 2015/2193. Its provisions relate to installations with a rated thermal input greater or equal to 1 MW and lower than 50 MW. New stricter limit values of NO<sub>x</sub>, SO<sub>x</sub> and particulate matter emissions for these installations are defined and should replace the currently valid limits stated in the *TA Luft*. Concurrently, the 1<sup>st</sup> ordinance shall be amended [26]. However, this 44<sup>th</sup> ordinance has not entered into force yet (April 2019).

Tab. 6: Emission limits [ $\text{mg}\cdot\text{m}^{-3}$ ] for installations with thermal input lower than 50 MW valid in Germany [24]

Fuel	NO <sub>x</sub>	CO
Untreated wood	250	150
Other solid fuels in fluidised bed furnace	300	
Other solid fuels, thermal input < 10 MW	500	
Other solid fuels, thermal input $\geq$ 10MW	400	
Oils defined in DIN 51603	180	80
Other liquid fuels	350	
Gaseous fuels from public gas supply	100	50
Other gaseous fuels	200	80

### 3.3.1 Thru.de

The regulation no. 166/2006/EC concerning establishment of E-PRT is in Germany implemented through an act referred as *SchadRegProtAG*<sup>16</sup>. The German national PRTR is named *Thru.de*<sup>17</sup> and it is run by German Environmental Agency (UBA)<sup>18</sup>. It provides data about 91 pollutants into air, water and soil, as well as information about waste transfers from ca. 5000 registered industrial facilities in Germany (5417 facilities in 2016). These pollutants are divided into seven groups: greenhouse gases, other gases, heavy metals, pesticides, chlorinated organic substances, other organic substances and inorganic substances [27].

The data from the facilities are collected in a three-step process. At first, the operators of the facilities forward the data to a competent authority in the corresponding federal state. These authorities review the data for completeness and plausibility and send it subsequently to the German Environmental Agency. In the last step, the UBA makes another review of the data and releases it on *Thru.de*. Concurrently forwards the UBA the data to the European Commission, which includes it in the European Pollution Release and Transfer Register [27]. In the Tab. 7, the top five NO<sub>x</sub> producers in Germany are listed, based on the data in *Thru.de* from year 2016.

Tab. 7: The top five NO<sub>x</sub> emissions producers in Germany, 2016 [28]

No.	Facility	Main activity	Federal state	NO <sub>x</sub> [t/y]
1.	RWE Power AG, Grevenbroich	Thermal power station	NRW	21 700
2.	LEAG, Kraftwerk Jänschwalde	Thermal power station	Brandenburg	19 200
3.	RWE Power AG, Kraftwerk Niederaußem	Thermal power station	NRW	16 500
4.	LEAG, Kraftwerk Boxberg	Thermal power station	Sachsen	13 300
5.	RWE Power AG, Eschweiler	Thermal power station	NRW	12 700

Note: NRW = Nordrhein–Westfalen

<sup>16</sup> Gesetz zur Ausführung des Protokolls über Schadstofffreisetzungs- und -verbringungsregister sowie zur Durchführung der Verordnung (EG) Nr. 166/2006

<sup>17</sup> The name refers to the Nordic goddess of trees and flowers *Thrude* [27]

<sup>18</sup> Umweltbundesamt

As a result of legislative measures, the air quality in the member countries of the EU has in recent decades significantly improved. This can be seen e.g. in Fig. 5, which shows a comparison of average yearly concentrations of  $\text{NO}_x$  in Germany between the years 1990 and 2015. Again, it is obvious that the highest concentrations were registered in large cities and in industrial regions, e.g. in western part of the country in the federal state Nordrhein–Westfalen. Nevertheless, there are also points with high  $\text{NO}_x$  concentration in the eastern part of Germany in Lausitz region, where several coal-fired power stations are located. In general, thermal power stations are one of the most significant sources of  $\text{NO}_x$  emissions. This fact can be supported by the list of the top  $\text{NO}_x$  producers in Germany (Tab. 7), based on data from *Thru.de*, since all the five top places are occupied by thermal power stations.

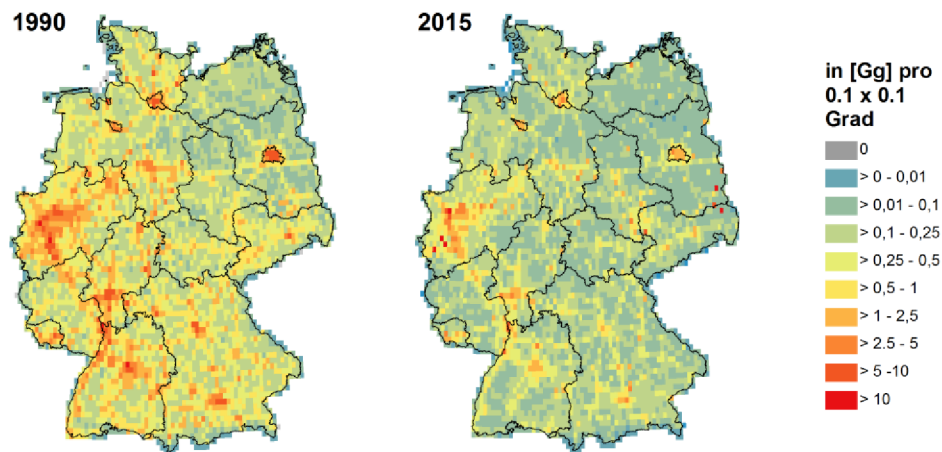


Fig. 5: Comparison of average yearly concentrations of  $\text{NO}_x$  in Germany in years 1990 and 2015 [29]



## 4 Heat transfer

Heat transfer is the crucial part of industrial combustion. In accordance with the second law of thermodynamics, heat is spontaneously transferred from places with higher temperature to places with lower temperature [30]. There are generally three mechanisms of heat transfer. All these mechanisms participate in the heat transfer simultaneously, but in some applications, there is one dominant mechanism. Thus, it may be possible to simplify the case by neglecting the minor mechanisms, which can make the necessary calculations easier. During combustion processes, radiation is the most important mechanism due to high temperatures, as described in chapter 4.3.

### 4.1 Conduction

The kinetic energy of disorganised particles movement is transferred by collisions between neighbouring particles of mass, which is also called *diffusion of energy* [5]. This can be described by the Fourier's law of heat conduction. For a general three-dimensional body, it can be written in following form [30]:

$$\vec{q} = -\lambda \cdot \text{grad } T \quad (4.1)$$

When considering only one-dimensional case, it is possible to write:

$$\dot{q} = -\lambda \cdot \frac{dT}{dx} \quad (4.2)$$

where  $\dot{q}$  is heat flux [ $\text{W}\cdot\text{m}^{-2}$ ],  $\lambda$  is thermal conductivity of the material [ $\text{W}\cdot\text{m}^{-1}\cdot\text{K}^{-1}$ ],  $T$  is thermodynamic temperature [K] and  $x$  is length coordinate [m]. The minus sign in these equations denotes, that the heat moves from places with higher temperature to the colder ones. Therefore, when the temperature gradient is positive, the heat flux must be negative. According to these equations (4.1) and (4.2), the heat flux is proportional to the temperature gradient. The proportionality constant is the thermal conductivity  $\lambda$  of the heat transferring material [5]. Its value is generally higher for solid materials than for liquid and gas ones. Therefore, conduction occurs especially in solid bodies.

### 4.2 Convection

Characteristic for convection is that particles of mass change their position in space and carry the heat energy. The convection can be either natural or forced. The natural convection occurs as a result of local density differences. In case of forced convection, the driving force is mechanical energy from devices such as fans or pumps [5].

The convection is described by the Newton's law of cooling [30]:

$$\dot{Q} = A \cdot \alpha \cdot (T_w - T_\infty) \quad (4.3)$$

where  $\dot{Q}$  is the heat flow rate [W],  $A$  is the heat transfer surface area [ $\text{m}^2$ ],  $\alpha$  is the heat transfer coefficient [ $\text{W}\cdot\text{m}^{-2}\cdot\text{K}^{-1}$ ],  $T_w$  is the temperature of the body surface [K] and  $T_\infty$  is the temperature of the environment [K].

The value of the heat transfer coefficient  $\alpha$  depends on six independent variables, namely: flow velocity  $u$  [ $\text{m}\cdot\text{s}^{-1}$ ], characteristic dimension  $L$  [m] (e.g. diameter of a pipe), and properties of the fluid: density  $\rho$  [ $\text{kg}\cdot\text{m}^{-3}$ ], kinematic viscosity  $\nu$  [ $\text{m}^2\cdot\text{s}^{-1}$ ], specific heat capacity  $c_p$  [ $\text{J}\cdot\text{kg}^{-1}\cdot\text{K}^{-1}$ ] and thermal conductivity  $\lambda$  [ $\text{W}\cdot\text{m}^{-1}\cdot\text{K}^{-1}$ ]. The relationship between these variables can be described by three dimensionless criteria: Nusselt number  $Nu$  (ratio of

convective to conductive heat transfer), Reynolds number  $Re$  (ratio of inertial forces to viscous forces) and Prandtl number  $Pr$  (ratio of momentum diffusivity to thermal diffusivity) [30].

$$Nu = \frac{\alpha \cdot L}{\lambda} \quad (4.4)$$

$$Re = \frac{u \cdot L}{\nu} \quad (4.5)$$

$$Pr = \frac{\nu \cdot \rho \cdot c_p}{\lambda} = \frac{\nu}{\alpha} \quad (4.6)$$

### 4.3 Radiation

In combustion processes, the predominant mechanism of heat transfer is radiation. It is the only mechanism which enables heat transfer in vacuum. Actually, it is a movement of energy by electromagnetic waves [5]. Therefore, the speed of propagation depends on type of the environment<sup>19</sup>. According to Stefan–Boltzmann law (4.7), the heat flow rate is proportional to the fourth power of thermodynamic temperature of the body. The constant of proportionality in this law is called Stefan–Boltzmann constant<sup>20</sup>. The Stefan–Boltzmann law<sup>21</sup> can be written in following form [5]:

$$\dot{Q} = \varepsilon \cdot A \cdot \sigma \cdot T^4 \quad (4.7)$$

where  $\dot{Q}$  is the heat flow rate [W],  $\varepsilon$  is emissivity [-],  $A$  is surface area of the body [m<sup>2</sup>],  $\sigma$  is the Stefan–Boltzmann constant [W·m<sup>-2</sup>·K<sup>-4</sup>] and  $T$  is the thermodynamic temperature [K]. The emissivity can be defined as a ratio of energy emitted from surface of a body to energy theoretically emitted from this surface at the same temperature if the body would be black<sup>22</sup>. For a black body, the emissivity is equal to one. On the contrary, for a white body is the emissivity equal to zero, however, these are only ideal cases. All real bodies can be described as grey bodies. Therefore, their values of emissivity lie between zero and one [30].

<sup>19</sup> In vacuum, the speed of propagation of electromagnetic waves is equal to  $c_0 = 2.998 \cdot 10^8 \text{ m}\cdot\text{s}^{-1}$  [5].

<sup>20</sup> Stefan–Boltzmann constant  $\sigma = 5.669 \cdot 10^{-8} \text{ W}\cdot\text{m}^{-2}\cdot\text{K}^{-4}$  [5]

<sup>21</sup> The Stefan–Boltzmann law is obtained by integration of the Planck's law over all wavelengths.

<sup>22</sup> A black body is an idealized body, which emits (and absorbs) the maximum possible amount of radiation energy for all wavelengths.

## 5 Types and classification of burners

The chemical energy of fuel is converted into thermal energy by combustion in burners. There are several ways how to classify industrial burners. In this chapter, burners are described according to four different criteria: mixing type, fuel type, oxidizer type and draft type.

### 5.1 Mixing type

#### 5.1.1 Diffusion burners

A commonly used method for classifying burners is according to how the fuel and the oxidizer are mixed. In a diffusion burner, the fuel meets combustion air outside the fuel nozzle without any previous mixing. By separating the fuel from the oxidizer before the ignition zone, the possibility of flashback is eliminated. Therefore, diffusion burners are able to handle a wide range of fuels without any concern on safety. Another major advantage of diffusion burners is their simple construction. They are commonly also referred as *raw-gas* or *nozzle-mix* burners [31].



Fig. 6: Schematic of a diffusion burner [5]

#### 5.1.2 Premixed burners

On the contrary, in premixed burners, the fuel and the oxidizer are completely mixed before the combustion starts. In comparison to diffusion burners, the flame is shorter and more intense. This leads to formation of high temperature regions, which causes less uniform distribution of temperature and heat flux across the flame but enables achieving higher peak temperature [31]. Nevertheless, higher temperature leads to increased formation of nitrogen oxides via the thermal mechanism [8].

Burners can be also partially premixed, which means, only a fraction of fuel is mixed with the oxidizer before the combustion. This is often done for improving combustion stability as well as for safety reasons since partial premixing reduces the risk of flashback. The properties of a partially premixed flame (i.e. length, peak temperature, uniformity of heat flux distribution) are somewhere between diffusion and premixed burners [5]. A schematic of a partially premixed burner can be seen in Fig. 8

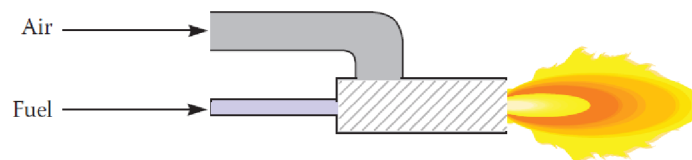


Fig. 7: Schematic of a premix burner [5]

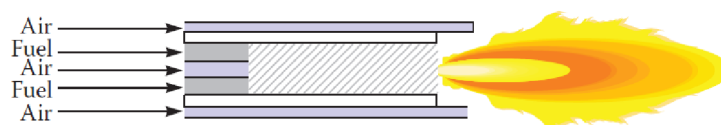


Fig. 8: Schematic of a partially premixed burner [5]

## 5.2 Fuel type

### 5.2.1 Gaseous fuel

Gaseous fuel is the dominant fuel source used in the process industry owing to good availability and low price of natural gas, which is the most widespread gaseous fuel. Natural gas consists of a wide range of hydrocarbons, with methane (70 to 99.6 % vol.) and ethane (2 to 16 % vol.) making up the majority [5]. In many industrial applications, a mixture of different gases (e.g. hydrogen, methane, propane etc.) is frequently used as fuel. Other reasons for using gaseous fuel are low emissions and low maintenance costs of equipment in comparison to other fuel types [6]. In general, gaseous fuels produce often nonluminous flames with a very small amount of soot particles. Another advantage of utilizing gaseous fuels is that they do not require any treatment before utilization, whereas liquid fuels need to be atomized and solid fuels need to be pulverized.

### 5.2.2 Liquid fuel

A key requirement for complete combustion of liquid fuels is their good atomisation into small enough droplets in order to achieve high combustion efficiency and low unburned hydrocarbon emissions. When designing the atomizer, several factors need to be considered, e.g. viscosity of the fuel as a function of temperature or vaporization temperature of the fuel [31]. The process of fuel atomization was experimentally investigated and more in detail described by Liu et al. [32]. Another drawback of burning liquid fuels is that they often contain bound impurities, especially sulphur, which causes formation of SO<sub>x</sub>, and nitrogen, which is responsible for formation of NO<sub>x</sub> emissions via the fuel mechanism [5].

Some burners are able to operate on more than one type of fuel, where one fuel is major, whereas the other fuels are used as a reserve in case of drop-out of the major fuel. It is also possible to switch between the fuels for economic reasons. An example of simultaneous burning of more fuel types can be waste incineration, where a waste liquid is fed to burner which is powered by an auxiliary fuel (usually natural gas). This is commonly done because of low heating values of the waste fuel [31].

### 5.2.3 Solid fuel

The utilization of solid fuels like wood has been known since the early civilization, nevertheless, this type of fuel is not very frequent in process industrial applications. The two most utilized solid fuels in these applications are coal (e.g. in power generation industry) and coke (e.g. in metal production). To burn coal in a burner, it is necessary to pulverize it before. Based on experimental investigation conducted by Liu et al. [33], preheating the pulverized coal is an effective way for reducing NO emissions for some types of burners. Another example of solid fuel is sludge, which is combusted in incineration plants. In general, industrial burners for solid fuels usually have an annular zone to inject pneumatically conveyed fuel into the furnace [5]. However, the combustion of solid fuels does not comprise the subject matter of this thesis and therefore is not analysed further.

## 5.3 Oxidizer type

### 5.3.1 Atmospheric air combustion

In most combustion processes, the atmospheric air is used as oxidizer. The air in Earth's atmosphere contains approximately 21 % of oxygen by volume. In some cases, the combustion air is blended with the combustion products. As an example may serve flue gas recirculation, which is commonly used as a method for reducing NO<sub>x</sub> emissions [5].

### 5.3.2 Oxygen-enhanced combustion

In some industrial applications where high temperatures are needed (e.g. glass production or metallurgy) contains the oxidizer more than 21 % vol.  $O_2$ . Other reasons for oxygen enhanced combustion are higher combustion efficiency and lower fuel consumption [31]. The main drawback of utilizing oxygen is its high cost. There is also a risk of equipment damage by the high temperatures. Other disadvantages are nonuniform distribution of heat flux along the flame, risk of flame disturbances and flashback and possibility of higher thermal  $NO_x$  production due to higher temperatures [34].

There are four basic ways how to mix the oxygen with the combustion air [31]. One method consists in injecting the oxygen into combustion air supply through a diffuser in order to achieve proper mixing, as can be seen in the Fig. 9 This is referred as *air enrichment*.

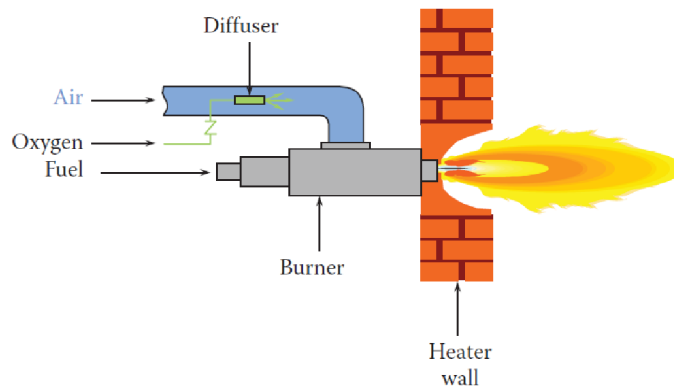


Fig. 9: Schematic of an oxygen-enriched air/fuel burner [5]

Another method *air-oxy/fuel* involves injecting  $O_2$  directly to the flame, separately from the air/fuel mixture. There is also possibility to inject oxygen into the combustion chamber without modifying the existing conventional air/fuel burner. This technique is called  *$O_2$  lancing* [5].

The influence of oxygen content in combustion air on the combustion characteristics was experimentally investigated more in detail by Bělohradský et al. [35] at a natural gas burner. The overall oxygen concentration was varied from 21 % to 46 %. It was observed that  $NO_x$  emissions in flue gas were higher with increasing  $O_2$  concentration. The  $NO_x$  formation was significantly lower for air-oxy/fuel combustion than for air enrichment method. Wu [36] et al. observed that amount of  $NO_x$  emissions increased 4.4 times when the overall  $O_2$  concentration was increased from 21 to 30 % due to higher furnace temperature.

In some processes, high-purity oxygen is utilized as the oxidizer. This is often referred as *oxy/fuel combustion*. The advantage of oxy-fuel combustion is a very low formation of thermal  $NO_x$ , because there is a low amount of nitrogen contained in the oxidizer. The only way how  $NO_x$  emissions may form during oxy-fuel combustion is from nitrogen bound in the fuel via the fuel mechanism [5]. A schematic of an oxy-fuel burner is shown in Fig. 10.

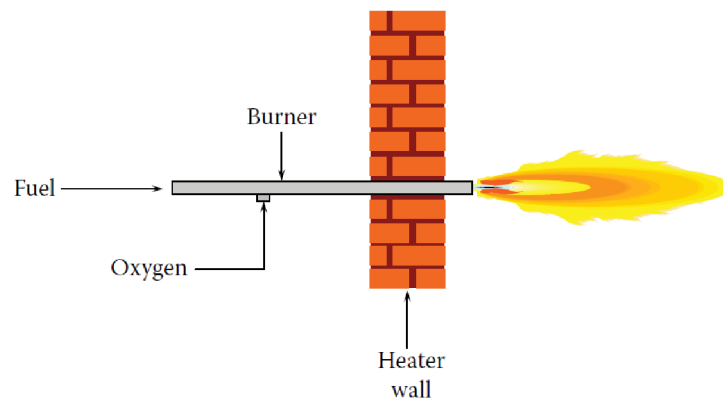


Fig. 10: Schematic of an oxy-fuel burner [5]

## 5.4 Draft type

Draft can be described as a driving force which enables the flow of the combustion air through the burner. According to API 535, it is possible to categorize burners into two categories based on the draft type [37].

### 5.4.1 Natural draft

In a natural-draft burner, the negative draft produced by the fuel jets is used for supplying the oxidizer to the burner. Therefore, it may be more difficult to control this burner type with regard to environmental conditions, as the operation can be negatively influenced by wind speed or humidity variations when operating the burner outdoor. The natural-draft flame is usually longer than the forced-draft one, which means the heat is distributed over a longer distance and therefore is also the peak temperature lower [31]. A typical use of natural-draft burners is in process heaters in chemical and petrochemical industry, where no rapid changes of thermal output are usually needed [5].

### 5.4.2 Forced draft

In case of forced-draft burners (sometimes referred as mechanical-draft burners [5]), the oxidizer is supplied to the burner at a positive pressure. This can be achieved by using a blower or a fan, which means higher capital cost of the equipment, as well as higher operation and maintenance costs. Most of the industrial burners use forced draft because of their higher combustion stability, wide range of thermal output and an easy control in comparison with natural-draft burners [31]. Forced-draft burners are often used with air preheating systems since fans are able to overcome the pressure drop across the preheater [37].

## 6 Combustion air preheating

Preheating the combustion air is often done in order to recover part of the energy from the exhaust products [31]. This results in a nearly linear increase of the adiabatic flame temperature, as can be seen in Fig. 11. The radiant heat flux increases with the fourth power of thermodynamic temperature according to the Stefan–Boltzmann law (4.7).

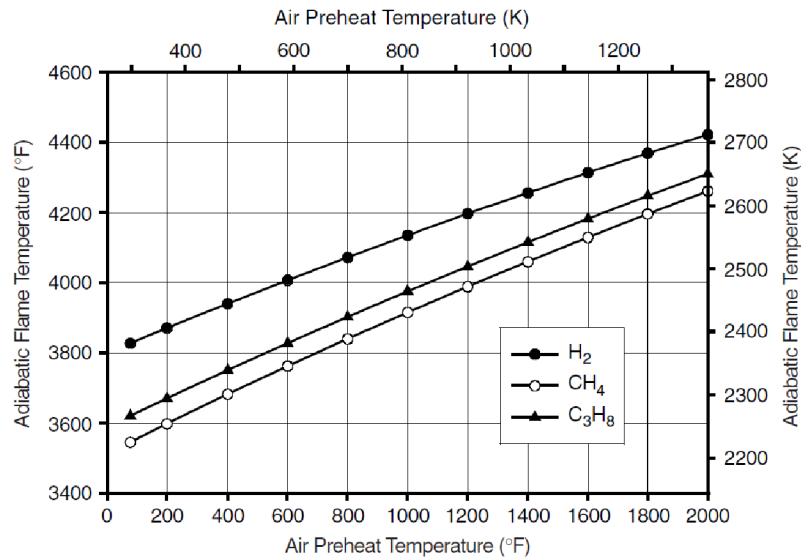


Fig. 11: Adiabatic flame temperature as a function of air preheat temperature for different fuels [31]

Another positive effect of preheating the combustion air (or oxidizer in general) is improving the thermal efficiency of the combustion process by increasing the available heat. The available heat is defined as higher heating value of the fuel minus the energy carried out of the exhaust stack by the flue gases. Fig. 12 shows an nearly linear increase of the available heat for three different fuels [31].

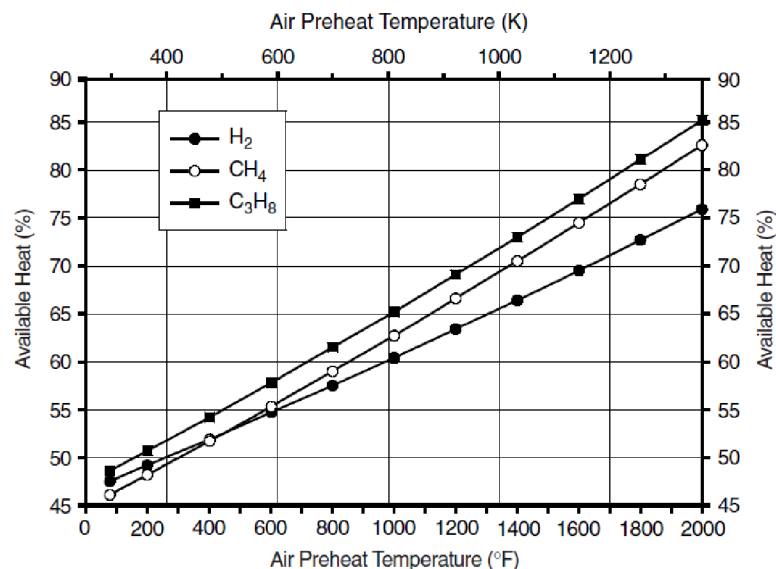


Fig. 12: Available heat as a function of air preheat temperature for different fuels [31]

On the other hand, higher temperatures in the combustion chamber achieved by combustion air preheating cause higher emissions of nitrogen oxides formed by the thermal mechanism, as described in chapter 2.1. The temperature dependence of NO emissions is depicted in Fig. 13 [5].

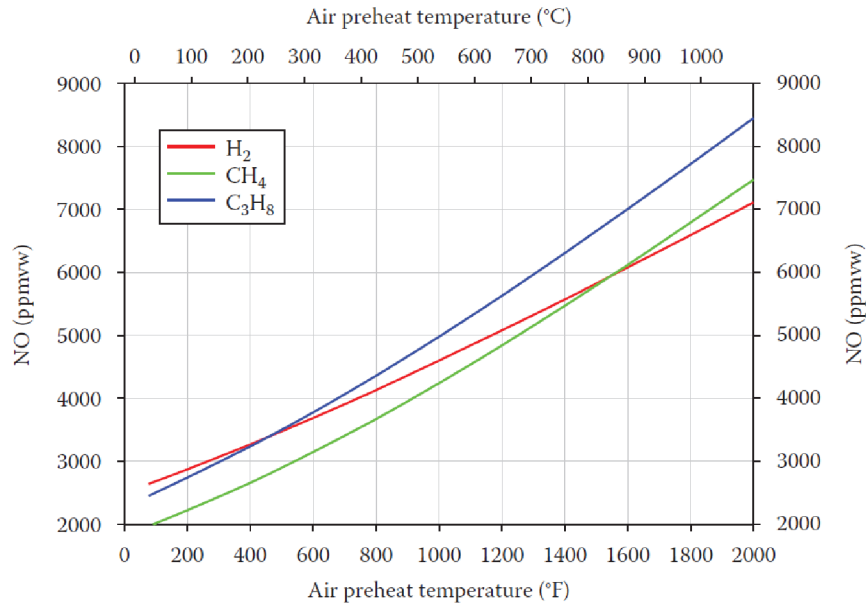


Fig. 13: Adiabatic equilibrium of NO emissions as a function of air preheat temperature for stoichiometric air/fuel flames [5]

Fig. 14 show the effects of combustion air preheating on carbon monoxide production. High flame temperatures achieved by preheating cause higher CO emissions as the preheat temperature increases [5].

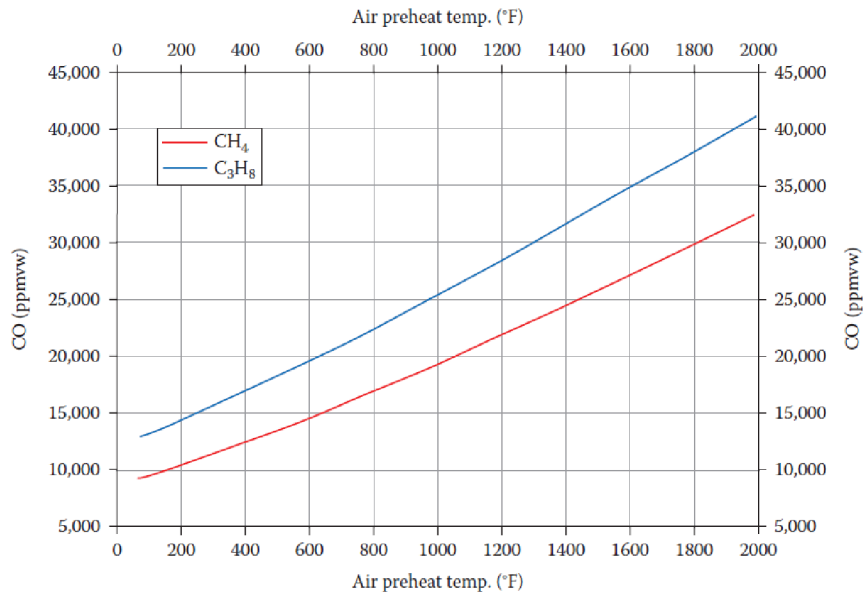


Fig. 14: Adiabatic equilibrium of CO emissions as a function of air preheat temperature for stoichiometric air/fuel flames [5]



## 6.1 Devices for preheating

The devices for heat recovery from flue gases to the combustion air can be divided into two basic categories: regenerators and recuperators.

### 6.1.1 Recuperators

Characteristic for recuperators in comparison to regenerators is the fact that the heat is transferred by conduction through a wall and the hot exhaust gases do not contact the same surface as the heated air. This is an advantage e.g. in case that the flue gases contain solid particles and a risk of combustion air contamination exists. A disadvantage of recuperators is a limited use at higher temperatures. For preheating temperatures up to 700 °C, recuperators made of metal can be utilized. Recuperators for preheating to higher temperatures require using ceramics instead of metals [31].

Heat recuperation is frequently done using external heat exchangers and does not involve the burners at all [5]. A commonly used recuperative air heater is the tubular type, but for lower air and flue gas pressures, the plate type can be also used. Tubular air heaters are commonly shell-and-tube type with a counter-current flow arrangement, where hot flue gases pass through the inside of the tubes and air flows outside. Baffles are provided to maximize the contact area between air and the hot tubes. Another disadvantage is that these heaters usually occupy a large space [7]. However, it is also possible to recuperate the waste heat using a recuperator integrated within the burner [38].

### 6.1.2 Regenerators

Regenerators are typically used in high-temperature processes, frequently over 1000 °C. Their working principle is that energy from the hot exhaust gases is temporarily stored in a unit constructed out of refractory firebricks. The material for the heat storage must be able to resist the high temperatures, for example some type of porous ceramic or alumina can be used. Another requirement on the burners in regenerative applications is that they must be able to work in periodical thermal cycles. Usually are the regenerators operated in pairs [31].

In the first part of the cycle flows the hot flue gas through one of the regenerators, while the cold combustion air is being heated up by the refractory bricks in the other regenerator. Both the combustion air and the flue gas are in direct contact with the bricks, although not both at the same time. After a certain time (mostly 5 to 30 minutes), when a certain temperature level is reached, the cycle is reversed: the bricks in the cold regenerator are reheated now by the flue gas, while the hot regenerator is cooled by the incoming combustion air [31]. In the temperature range from 800 to 1400 °C, 90 % of the heat from the flue gases can be transferred to the incoming combustion air. This enables to reach up to 80 % gross thermal efficiency [38].

An example of regenerative burners utilization is a method for NO<sub>x</sub> reduction called HiTAC (High Temperature Air Combustion) which leads to more uniform temperature field in the furnace. The formation of NO<sub>x</sub> occurs then predominantly by the prompt mechanism. This method, characterized also by low oxygen concentration, was investigated more in detail by e.g. Rafidi and Blasiak [39].

## 6.2 Previous research

Suzukawa et al. [40] carried out tests of a newly developed regenerative fuel-staged burner where the primary fuel comprised 10 to 15 % of the total fuel. A ceramic honeycomb was used as heat storage medium, that was able to raise the combustion air temperature up to 1300 °C, which was close to the furnace gas temperature 1350 °C. The fuel was a mixture of gases (N<sub>2</sub> 26.4 %, CO 25.2 %, H<sub>2</sub> 23.5 %, CH<sub>4</sub> 11.1 % vol.) with a lower heating value of 11.5 MJ·mN<sup>-3</sup>. The air excess ratio was kept constantly 1.05 throughout the experiment. The NO<sub>x</sub> emissions were lower than 50 ppm (at 11 % O<sub>2</sub>), while temperature distribution in the furnace was quite uniform. Carbon monoxide was not detected in the flue gas.

Moreover, theoretical and numerical analyses on heat transfer improvement by highly preheated air combustion were carried out. A uniform gas temperature field can according to the authors increase the radiative heat transfer and contribute to saving of fuel. Fig. 16 shows the calculated results. For a preheated air temperature of 1000 °C, the fuel savings can be about 40 % compared to systems without preheating. With the newly developed system, it is possible to save approximately 10 to 15 % fuel in comparison to conventional preheating furnaces equipped with recuperators [40].

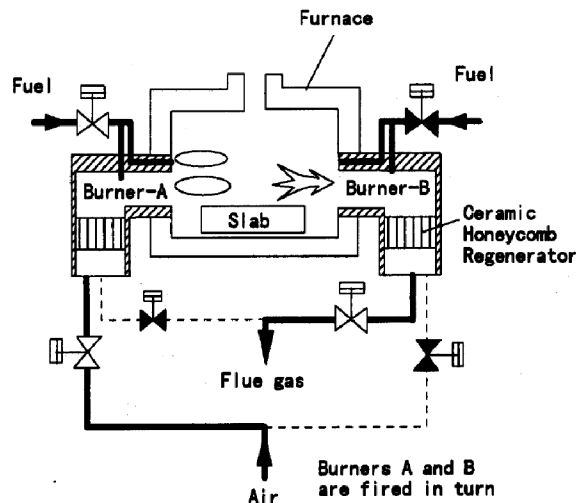


Fig. 15: Schematic diagram of the regenerative burner system [40]

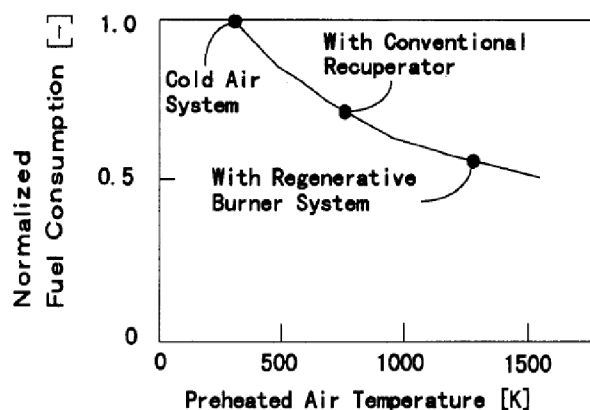


Fig. 16: Predicted fuel consumption improvement by combustion air preheating [40]

In another experimental study carried out by Sorrentino et al. [41], a combustion process in a cyclonic burner operated under MILD<sup>23</sup> conditions was investigated. During the tests, propane was used as fuel, the mixture equivalence ratio was constantly equal to 0.8, thermal power of the burner was fixed to 2 and 4 kW. Measurements of temperature at three different locations ( $T_1$ ,  $T_2$  and  $T_3$ ) inside the combustion chamber proved, that as air preheat temperature increased, temperatures in the chamber increased with an almost linear trend, as shown in Fig. 17. The decreasing difference between temperatures in particular locations suggested a higher uniformity of the temperature field with increasing preheat temperature.

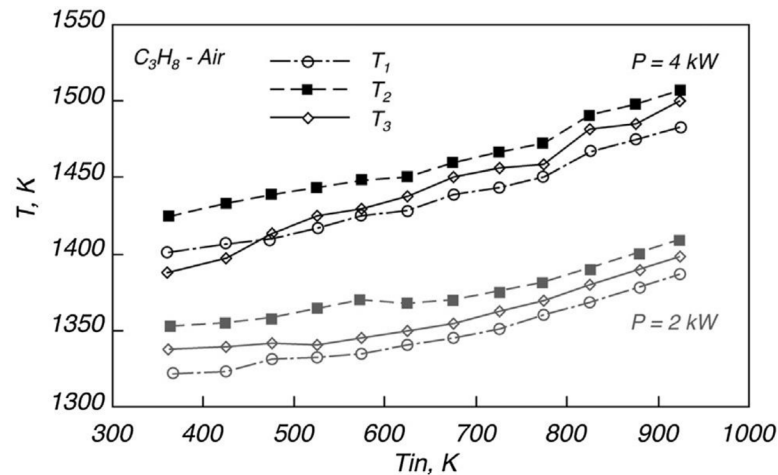


Fig. 17: Temperatures at three different locations in the chamber ( $T_1$ ,  $T_2$  and  $T_3$ ) as a function of combustion air temperature [41]

The experimentally obtained CO and  $\text{NO}_x$  emissions as a function of combustion air temperature are depicted in Fig. 18. Emissions of carbon monoxide slightly decreased from 10 to 5 ppm when the temperature increased up to 650 °C, while  $\text{NO}_x$  emission remained almost constant for the 2 kW-case. For the 4 kW-case, CO decreased from 16 to 10 ppm whereas the  $\text{NO}_x$  increased to 30 ppm while preheating the combustion air to 650 °C compared to 24 ppm without preheating [41].

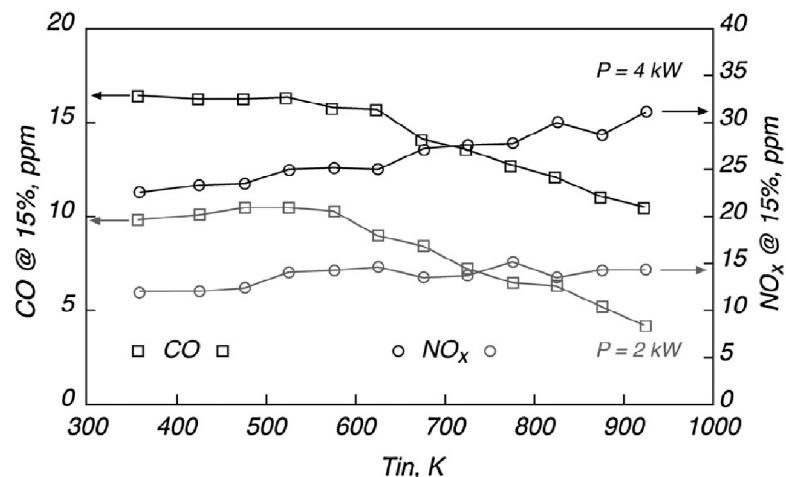


Fig. 18: CO and  $\text{NO}_x$  emissions as a function of combustion air temperature [41]

<sup>23</sup> Moderate or Intense Low-oxygen Dilution

The effect of air preheat temperature on MILD combustion of coal-derived syngas under the heat loads between 15.3 and 29.9 kW in a parallel jet forward flow combustor was investigated by Huang et al. [42]. The results showed that air preheating led to higher  $\text{NO}_x$  at a fixed equivalence ratio, as depicted in Fig. 19 a). This was caused by higher peak flame temperature. Lower carbon monoxide emissions were at a fixed equivalence ratio observed for the case with preheating (see Fig. 19 b)). According to the authors, this was related to the higher peak flame temperature combined with the longer reactants residence time in the high temperature region. The carbon monoxide had thus more time to accomplish the oxidation process.

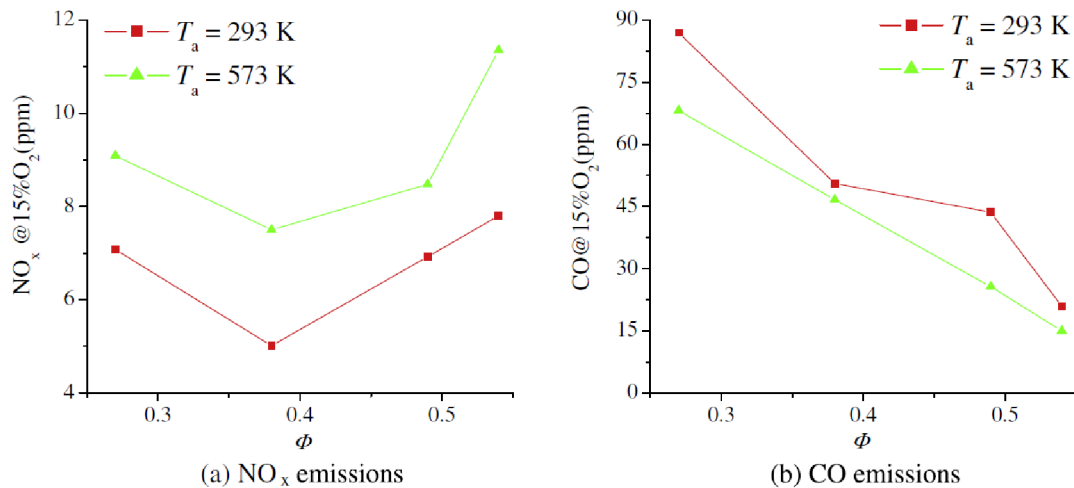


Fig. 19:  $\text{NO}_x$  and CO emissions at different combustion air temperatures as functions of equivalence ratio [42]

The structure of turbulent diffusion propane flames with highly preheated combustion air was experimentally investigated by Gupta et al. [43]. The test facility consisted of two combustion chambers, each of them was equipped with a ceramic honeycomb regenerator. The combustion air supplied to the test section was preheated to temperatures ranging from 900 to 1100 °C. At a standard concentration of oxygen in the combustion air 21 % vol., the following results were obtained: The flame volume and length as well as the content of yellow colour in the flame were found to increase with increasing preheat temperature. At 1100 °C, the flame was completely yellow. On the other hand, there was no yellow colour present in the flame at temperatures lower than 1000 °C. In contrast to this, the content of blue colour decreased at higher temperatures. This may suggest an increasing carbon production in the flame. Correspondingly, emission spectroscopy showed increasing concentrations of  $\bullet\text{OH}$ ,  $\text{CH}\bullet$ , and  $\text{C}_2$  at higher air preheat temperatures. It was demonstrated that thermal and chemical behaviour of the flame strongly depended on the preheating temperature.

## 7 Experimental investigation

### 7.1 Burner testing facility

An essential prerequisite for burner testing is a facility equipped with proper measuring instrumentation. The experimental investigation was carried out at large-scale burner testing facility located at Institute of Process Engineering, Faculty of Mechanical Engineering, Brno University of Technology. This facility is used for testing and research of industrial burners. It is possible to test gaseous, liquid and dual fuel burners [44].



Fig. 20: Burner testing facility at Institute of Process Engineering [44]

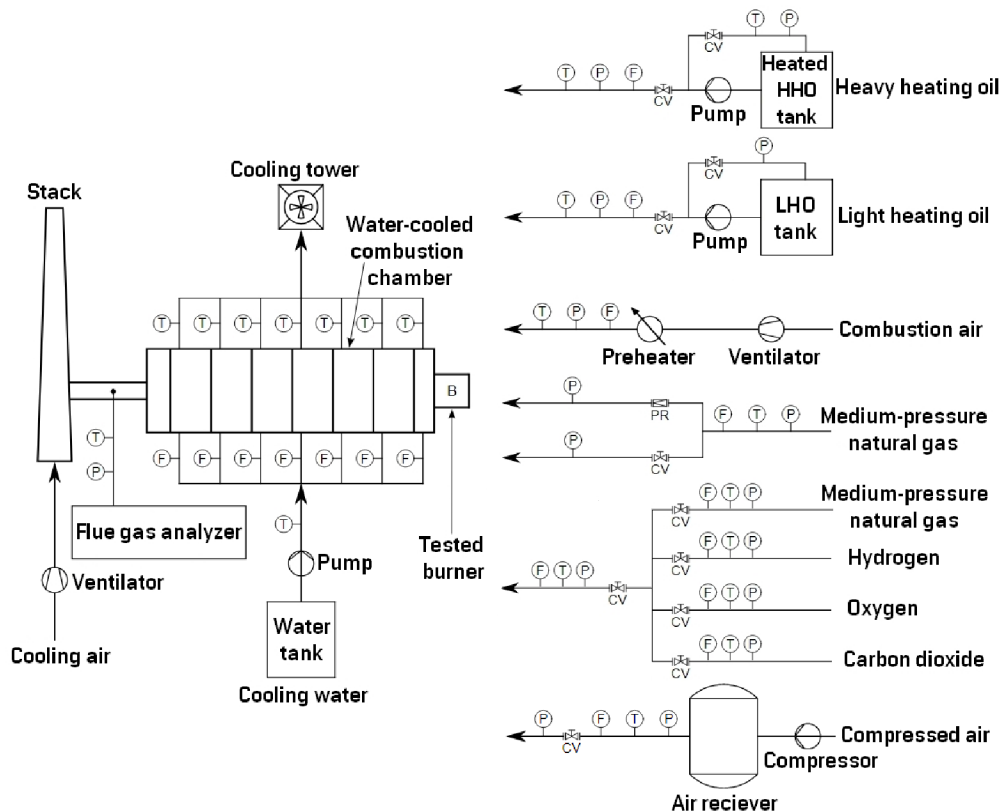


Fig. 21: Simplified block diagram of the burner testing facility. From [45], modified.

### 7.1.1 Combustion chamber

An important part of this facility is a horizontally oriented two-shell water-cooled combustion chamber with an inner diameter of 1 m and a length of 4 m. The water-cooled shell is divided into seven cylindrical sections with an independent water supply in each section. Moreover, each section is equipped with monitoring of inlet and outlet water temperatures and with water flow rate measurement. This enables to evaluate the heat fluxes from the hot flue gas to the shell. The hot water from the shell is cooled down in a cooling tower [44].

The six sections closest to the burner are 0.5 m long, the last section has a length of 1 m. Nevertheless, the first and the last section are insulated with a 100 mm thick high temperature fibrous lining. This means, the actual length of the heat transfer area is equal to 0.4 m in the first section closest to the burner and 0.9 m in the last seventh section [35]. In each section, there is a helix between the two shells, which is welded to the inner shell. The cooling water flows along a helical trajectory in order to avoid non-uniform heat fluxes in the particular sections. However, it was not possible to weld the helix to both inner and outer shell for fabrication reasons. Therefore, there is a small orifice between the helix and the outer shell, causing a short-circuit water flow, as can be seen in the Fig. 22 [46].

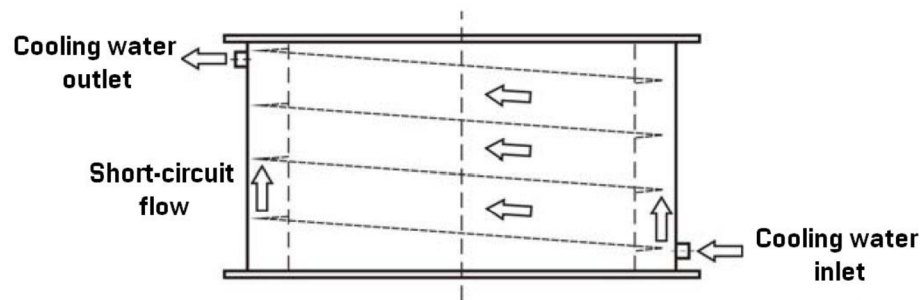


Fig. 22: Schematic of the helix and of the water flow in one section [46]

There are eighteen inspection holes in the chamber – eight holes on both sides of the cylindrical shell and two holes on the side opposite to the burner. These holes allow observation of the flame and installation of additional instrumentation, for example thermocouples for measuring temperature in the flame. The combustion chamber can be operated in both underpressure and overpressure regime. It is possible to change the pressure in a range from  $-300$  to  $800$  Pa with respect to the ambient pressure. The chamber is connected to a natural gas streamline capable of overpressure ranging from  $90$  up to  $105$  kPa. It is also possible to mix alternative fuels in the mixing station, which is able to mix up to four different gases.

The combustion air is supplied by a high-speed fan with a capacity of  $2500 \text{ m}_N^3 \cdot \text{h}^{-1}$ , where the overpressure behind the fan is ca.  $11.2$  kPa. Temperature, pressure and volume flow rate of the combustion air are measured at the inlet pipeline [44].

### 7.1.2 Combustion air preheater

It is also possible to preheat the combustion air. The preheater, which is situated outside the building, is composed of two parts – a jacketed combustion chamber and a convection block. The vertical combustion chamber is installed over the convection block on a steel construction. Supply of the heat for the combustion air preheating is provided by a natural gas burner APH-M 10 PZ manufactured by PBS Power Equipment [47]. The combustion air is supplied to the jacket of the combustion chamber by a radial fan. Inside the jacket, the air flows through a helical duct. The inlet and outlet of the air are arranged tangentially to the chamber (see Fig. 23) [48].

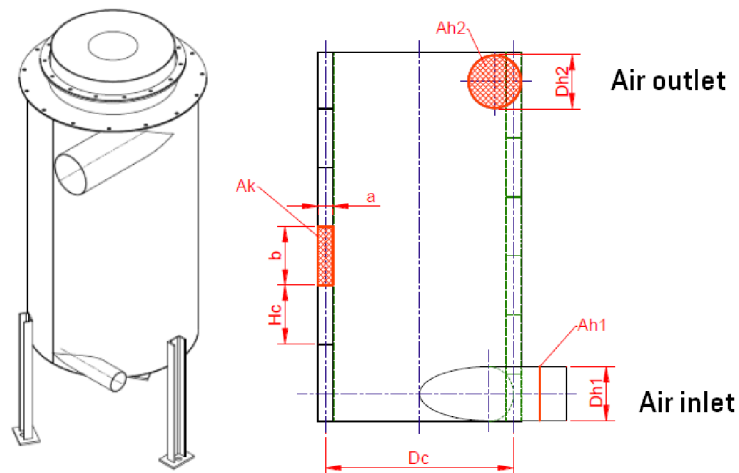


Fig. 23: View of the jacketed combustion chamber for air preheating [48]

At the outlet from the jacket, the air can be preheated up to 230 °C. Then, both the flue gas and preheated air flow through the convection block, which is anchored on a concrete footing. It is a shell and tube heat exchanger composed of three sections of U-tubes. These tubes are located in a housing equipped with a lining inside. The flue gas flows inside the tubes. After leaving the convection block, the flue gas goes on to the stack. The preheated combustion air flows outside the tubes through a system of baffles, so that the arrangement of the heat exchanger is purely counter-current (Fig. 24). The convection block enables to reach the temperature of the combustion air up to 500 °C [48].

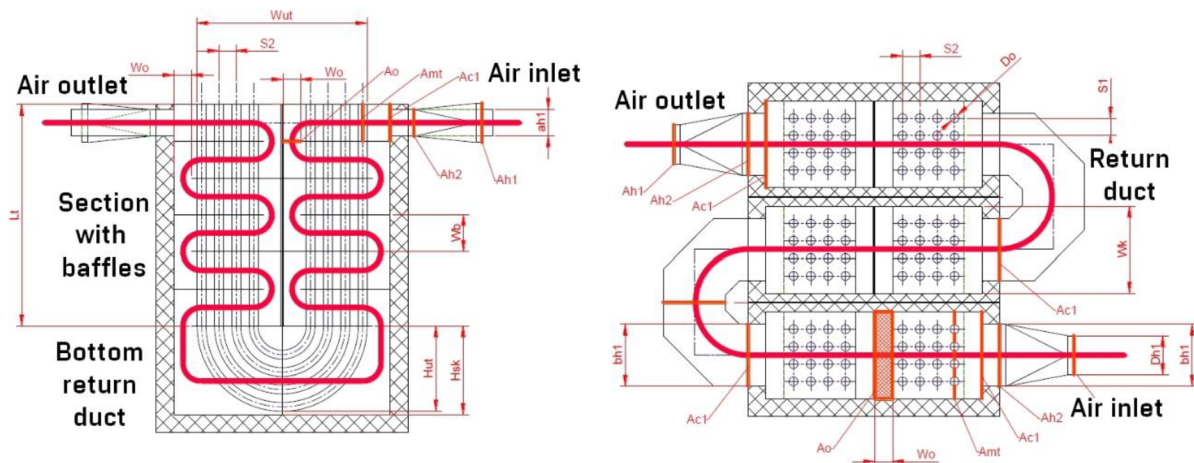


Fig. 24: Longitudinal and transversal cross-sections of the convection block [48]

### 7.1.3 Measurement instrumentation

The flue gas analysis is provided by a TESTO 350 XL flue gas analyser, equipped with electrochemical sensors for real-time measurement of O<sub>2</sub> (measuring range from 0 to 25 % vol.), CO (0 to 1000 ppm), NO (0 to 3000 ppm), NO<sub>2</sub> (0 to 500 ppm), SO<sub>x</sub> (0 to 5000 ppm) and C<sub>x</sub>H<sub>y</sub> (0 to 40000 ppm). Flue gas temperature is measured by a K-type thermocouple. Moreover, other types of external analysers can be installed into the chamber for measuring e.g. emissions of solid particles [44].

The testing facility is equipped with a safety system for a safe and reliable operation. This system consists of an ionization flame safeguard. In case of flame blow-off, the environment is no more ionized and the flame safeguard relay disconnects [49].

The user interface of the facility (Fig. 25) enables to regulate both the fuel and the combustion air flow rate fed to the burner. It is also possible to read all the instantaneous values of the measured quantities (temperature, pressure, flow rate, concentration) on the screen.

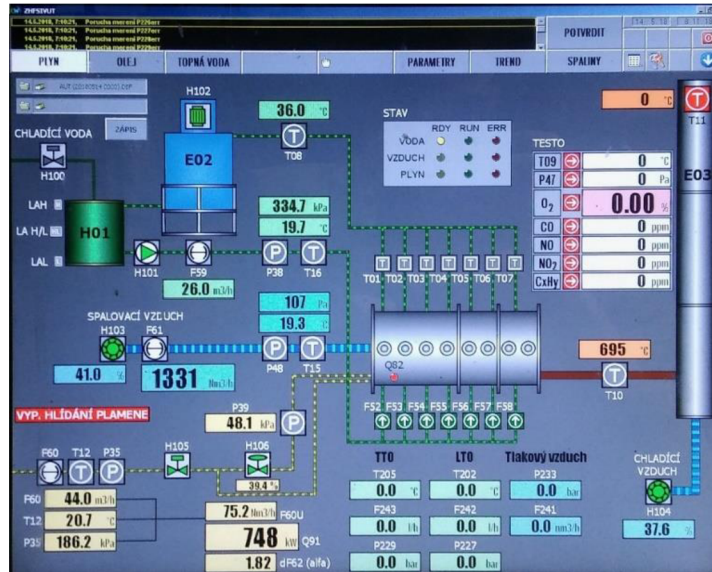


Fig. 25: User interface of the burner testing facility

Temperatures inside the combustion chamber can be measured by high-speed water-cooled R-type thermocouples, which are inserted into the inspection holes at each section of the chamber, as seen in the Fig. 26. The data is sent to a Graphtec midi GL220 datalogger.



Fig. 26: Detail of thermocouples for measuring temperatures in the combustion chamber

## 7.2 Burners

The experimental investigation was performed with two types of burners: a fuel-staged burner and a fuel-staged burner with integrated flue gas recirculation. These burners are described in the following chapters 7.2.1 and 7.2.2.

### 7.2.1 Fuel-staged burner

This burner is fired by natural gas, which is supplied to the burner in two stages. The combustion air supply is one-staged. It is a diffusion burner; the fuel and the combustion air are supplied separately and are not premixed before the combustion. The maximum thermal



input is 1500 kW. Diameter of the burner body, through which the combustion air is fed to the burner, is equal to 300 mm, same as the inner diameter of the burner quarl. There are two circular sets of primary fuel nozzles in the primary nozzle head. The first set contains four nozzles with a diameter of 3.0 mm whereas the other set consists of eight 2.6 mm nozzles [35].

The secondary fuel inlet is provided by four nozzle heads. Each of them contains two fuel nozzles. It is possible to change the tangential orientation of the secondary nozzle heads and their position in radial direction towards to the burner axis. However, the geometry of the burner was not changed during the tests. The influence of the secondary fuel nozzles setting on characteristic parameters of combustion was investigated e.g. by Macenauerová [49].

Moreover, it is possible to change the ratio of fuel supplied to the primary stage by placing an exchangeable orifice into the primary fuel inlet. The thermal input to the primary stage increases with the orifice diameter.

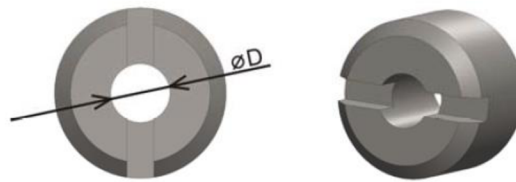


Fig. 27: 3D model of the exchangeable orifice for regulating fuel supply to the primary stage [35]

The burner is equipped with a flame holder, which has a form of a swirl generator consisting of eight pitched blades. This swirl generator is mounted on the central burner pipe. It provides tangential velocity to the combustion air, which leads to an intense mixing of the primary fuel with the air. Moreover, it prevents the flame blow-off. The flame ignition is provided by an auxiliary natural-draft premixed burner with a thermal input of 18 kW [35].

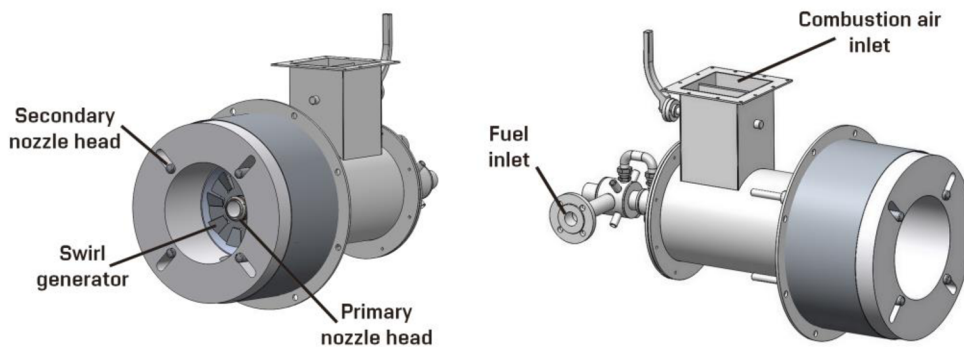


Fig. 28: 3D model of the fuel-staged burner [50]

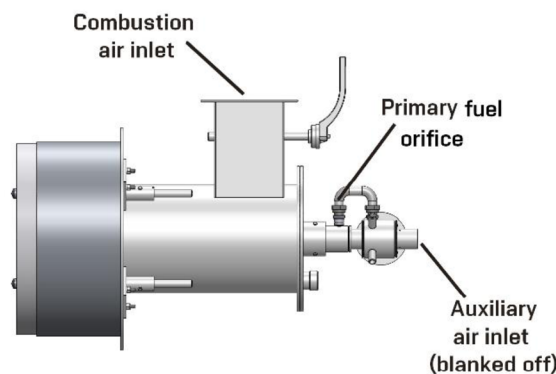


Fig. 29: Side view of the fuel-staged burner [50]

### 7.2.2 Fuel-staged burner with internal recirculation

The construction of this burner is similar to the fuel-staged burner described in chapter 7.2.1. It is a low-emission diffusion burner with a maximum thermal input of 1500 kW. The inner diameter of the burner quartz is 300 mm, the outer diameter is equal to 600 mm.

In comparison to the fuel-staged burner, there is one major difference in the construction. This burner includes a special device<sup>24</sup> for suction of the flue gas from the combustion chamber back to the burner body through four circular ducts.

The primary fuel nozzles are arranged in two circular sets. There are four nozzles with a diameter of 2.3 mm in the inner set and twelve nozzles with the same diameter in the outer set. In the secondary stage, the fuel is supplied to four adjustable nozzle heads [49].

It is possible to regulate the thermal input to the primary stage by using an exchangeable orifice, same as by the fuel-staged burner. The swirl generator as well as the auxiliary burner for ignition are the same as by the previous burner.

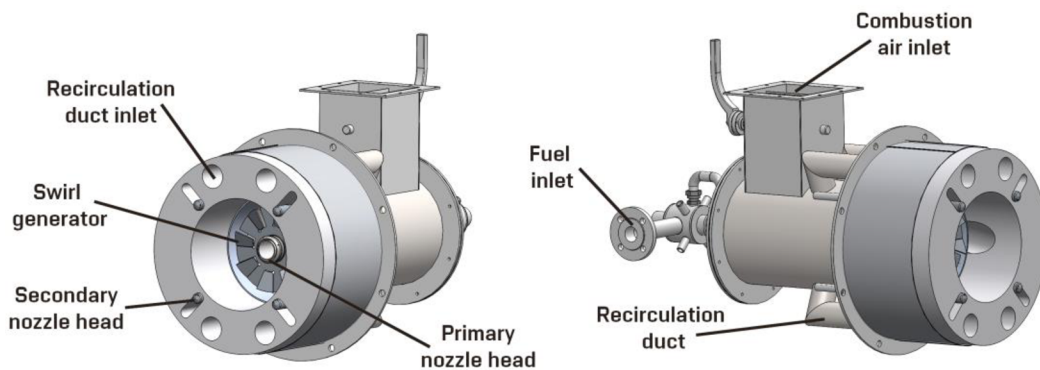


Fig. 30: 3D model of the fuel-staged burner with internal recirculation [50]

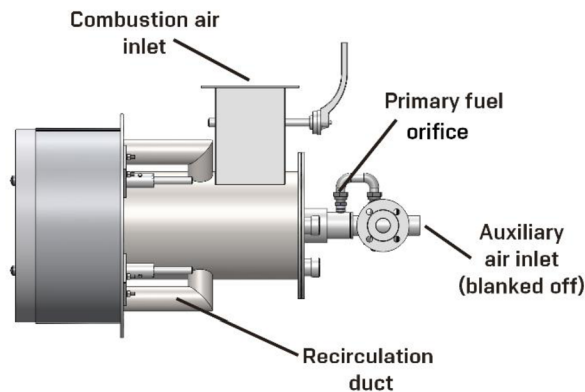


Fig. 31: Side view of the fuel-staged burner with internal recirculation [50]

## 7.3 Experimental setup

Throughout all the tests, natural gas was used as fuel. The thermal input to the burner was maintained at a constant value of 750 kW. This was done by regulating the amount of supplied fuel. The amount of combustion air fed to the burner was regulated so that the concentration of oxygen in the flue gas was constantly equal to 3 % by volume on dry basis.

<sup>24</sup> This device cannot be described more in detail due to protection of intellectual property.

During tests of the fuel-staged burner, the orifice with inner diameter of 4.5 mm was used. Tests of the burner with integrated recirculation were carried out with two different diameters of the orifice, namely 4.5 mm and 6.5 mm. During tests of the recirculating burner, the 6.5 mm orifice was used at first due to expected lower combustion stability with the 4.5 mm orifice, based on previous results obtained by Bělohradský [46]. However, the combustion was stable even with the smaller orifice diameter, as described in chapter 8.7.

In a temperature range of the combustion air from 20 to 250 °C, following parameters were investigated: NO<sub>x</sub> and CO emissions, flue gas temperature, heat fluxes from the combustion chamber to the shell, temperature distribution across the chamber, thermal efficiency of the radiant section, flame colour and stability. Heat fluxes and temperature distribution were measured at selected temperatures 20, 50, 150 and 250 °C. The emissions and temperature of flue gas were recorded in a step of 50 °C, in the range from 100 °C to 50 °C was the step size reduced to 10 °C. Moreover, temperature of the recirculated flue gas was measured in the recirculation duct at the recirculating burner. The flame stability was observed in a step of 50 °C.

The first measurements were carried out with non-preheated combustion air at a temperature of 20 °C. Then, the air was preheated to 250 °C. After reaching this target temperature and measuring all the parameters, the auxiliary preheater burner was switched off. Thus, the combustion air temperature was decreasing back to the ambient temperature. During this decreasing of the combustion air temperature, measurements at remaining temperatures were performed. These measurements required repeated short-time ignition of the preheater burner in order to reach a steady thermodynamic state.

## 8 Results

### 8.1 NO<sub>x</sub> emissions

The flue gas analyser provided values of NO, NO<sub>2</sub> and NO<sub>x</sub> concentrations in the flue gas. The provided concentration of NO<sub>x</sub> can be also calculated from the measured values of NO and NO<sub>2</sub> using the following equation:

$$\text{NO}_x [\text{mg} \cdot \text{m}^{-3}] = \text{NO} [\text{mg} \cdot \text{m}^{-3}] \cdot \frac{M(\text{NO}_2)}{M(\text{NO})} + \text{NO}_2 [\text{mg} \cdot \text{m}^{-3}] \quad (8.1)$$

The first term on the right side of the equation (8.1) is the measured NO concentration expressed as an equivalent concentration of NO<sub>2</sub>. Because the concentrations of NO and NO<sub>2</sub> were measured in ppm units, it was necessary to convert them into mg·m<sub>N</sub><sup>-3</sup>. This was done using the formula (8.2), which is valid for concentration of any general substance X. For converting into mg·m<sub>N</sub><sup>-3</sup>, the value of standard molar volume is  $V_M = 22.4136 \cdot 10^{-3} \text{ m}^3 \cdot \text{mol}^{-1}$  [30].

$$X [\text{mg} \cdot \text{m}^{-3}] = X [\text{ppm}] \cdot \frac{M(X)}{V_M} \quad (8.2)$$

The resulting dependences of NO<sub>x</sub> emissions on the combustion air temperature are shown in Fig. 32 for all three investigated burner settings.

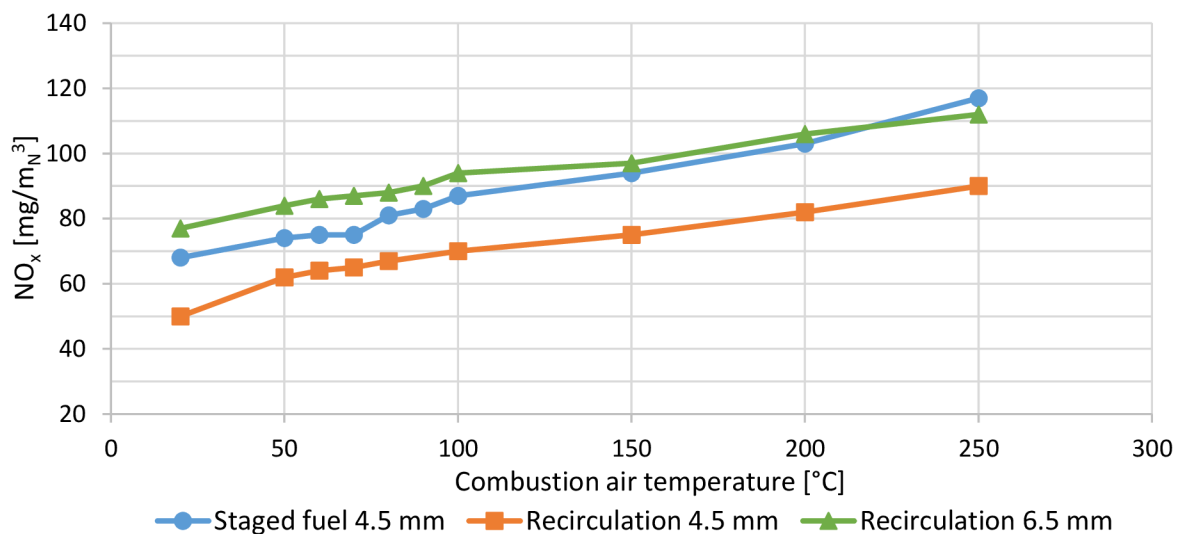


Fig. 32: Dependence of NO<sub>x</sub> concentrations in the flue gas on combustion air temperature

As can be seen from Tab. 2 and Tab. 6 in chapter 3, the limit values of NO<sub>x</sub> both in the Czech Republic and in Germany are equal to 100 mg·m<sub>N</sub><sup>-3</sup>. During the tests of the recirculating burner with the 4.5 mm orifice, NO<sub>x</sub> emissions were in compliance with the valid legislation across the whole investigated temperature range. For the other two configurations, the limit of 100 mg·m<sub>N</sub><sup>-3</sup> was exceeded when the combustion air temperature was higher than 150 °C.

As it is obvious, the NO<sub>x</sub> emissions increased with the combustion air temperature. Higher temperatures in the flame contribute to the increased formation of thermal NO<sub>x</sub>, which is the predominant mechanism of NO<sub>x</sub> formation during natural gas combustion. This is completely in accordance with the theory presented by Baukal [5].

It was investigated that  $\text{NO}_x$  emissions were lower with the smaller orifice diameter, which means a higher amount of fuel supplied to the secondary stage. This is an evidence that fuel staging is an effective method for reducing  $\text{NO}_x$  emissions, based on creating non-stoichiometric zones. It can be also observed from the temperature profiles in chapter 8.6 that distributing more fuel to the primary stage leads to the formation of high-temperature peaks in the burner vicinity, resulting in higher  $\text{NO}_x$  emissions.

During the tests of the fuel-staged burner, a 4.5 mm orifice was used. It was also found out that lower emissions were achieved at the fuel-staged burner without recirculation than at the fuel-staged recirculating burner with higher orifice diameter. Hence, increasing the ratio of fuel distributed to secondary stage seems to be more efficient way to reduce  $\text{NO}_x$  emissions than recirculating the flue gases without changing the orifice diameter. On the other hand, more fuel distributed to the secondary stage may have a negative impact on combustion stability (see chapter 8.7).

In case of using the same orifice diameter 4.5 mm,  $\text{NO}_x$  were lower at the recirculating fuel-staged burner than at the pure fuel-staged one. Recirculation of flue gas is a widely used primary method for reduction of  $\text{NO}_x$  based on flame cooling. It can be seen from temperature profiles in chapter 8.6 that the recirculation results in a more uniform temperature distribution across the chamber. Therefore, there are less high-temperature peaks which has a positive influence on  $\text{NO}_x$  reduction compared to the pure fuel-staged burner.

## 8.2 CO emissions

During all the tests carried out at oxygen concentration 3 % vol. in dry flue gas, CO emissions were very low (0 to  $3 \text{ mg}\cdot\text{m}_N^{-3}$ ). This was a sign of a complete combustion, which corresponds with the fact that air surplus was used. Throughout all tests, the legislative limit of  $50 \text{ mg}\cdot\text{m}_N^{-3}$  valid both in Germany and in the Czech Republic was not exceeded (for the limits see Tab. 2 and Tab. 6 in chapter 3). In general, it is possible to observe the trend that carbon monoxide emissions increase with higher combustion air temperature, which is in accordance with Baukal [5] (see chapter 6). The probable reason is the shorter residence time in the combustion chamber which may be insufficient for a complete combustion due to higher flow velocities at higher air temperatures, as already mentioned in chapter 2.4.

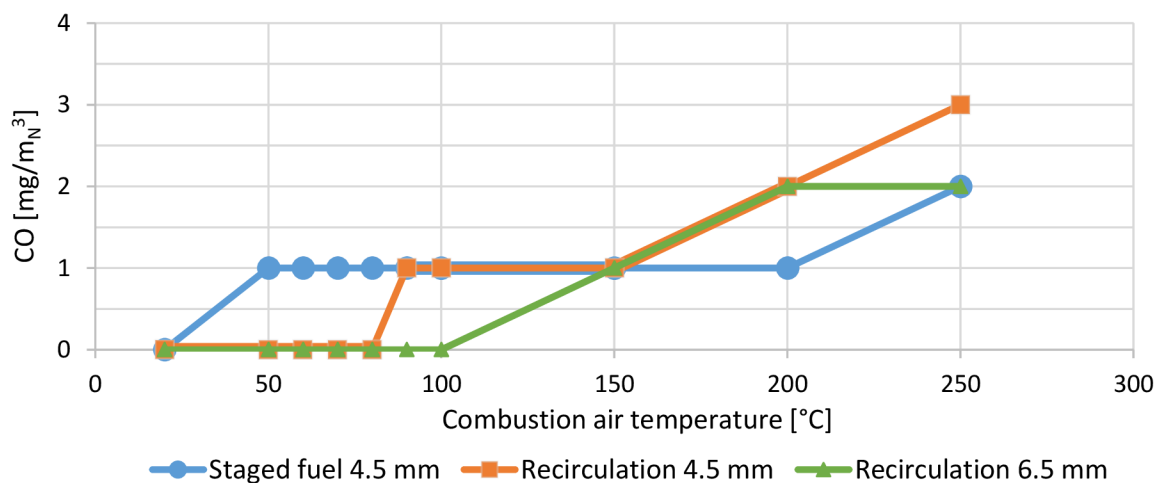


Fig. 33: Dependence of CO concentrations in the flue gas on combustion air temperature

### 8.3 Flue gas temperature

Temperatures of the flue gas were measured in the flue gas duct behind the outlet from the combustion chamber. The measured values are presented in Fig. 34.

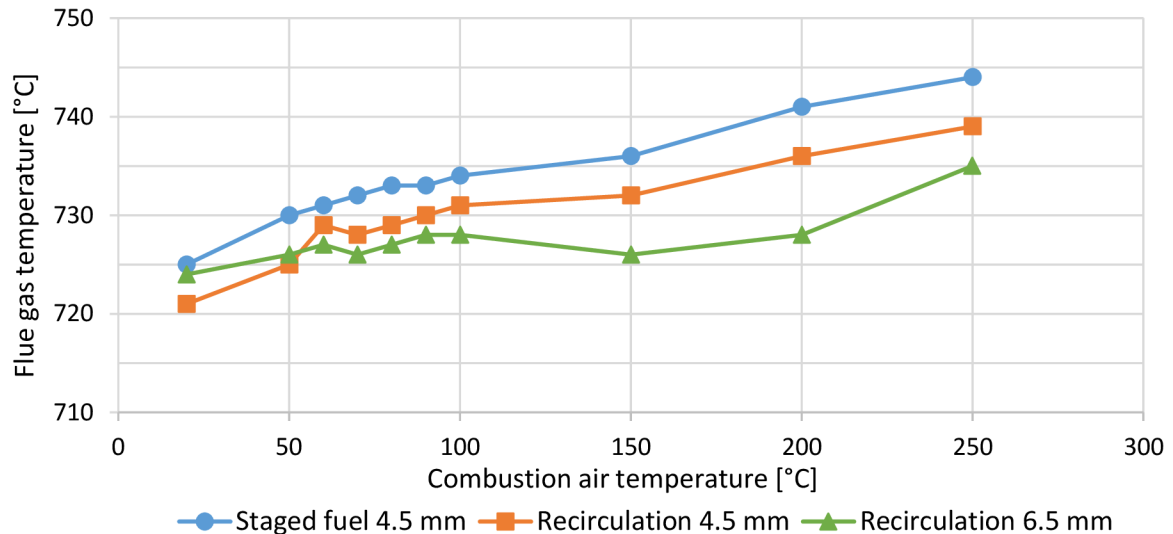


Fig. 34: Dependence of flue gas temperature on combustion air temperature

It was revealed that the influence of combustion air temperature on flue gas temperature was rather minor. Flue gas temperature was slightly increasing with the combustion air temperature as expected. However, the difference between flue gas temperatures for non-preheated air and air preheated to 250 °C was lower than 20 °C for all settings. The reason is that the enthalpy of the air is considerably lower than the energy released by combustion of the fuel (as calculated in chapter 8.5). Moreover, a part of the additional heat energy is recovered to the shell, which results in higher efficiency of the radiant section (chapter 8.5) The lowest flue gas temperatures for preheated combustion air were achieved using the recirculating burner with a 6.5 mm orifice. On the contrary, the highest flue gas temperatures were recorded for the fuel-staged burner.

In a previous experimental investigation by Hudák [51] carried out at a fuel staged burner with higher oxygen concentration and without recirculation, the flue gas temperature was increasing with larger diameter of the orifice. This is in contradiction with the above presented results for a recirculating fuel-staged burner. The possible explanation is that smaller diameter means more fuel distributed to the secondary stage. This results in higher temperatures near the secondary fuel nozzles (as can be seen from temperature profiles shown in chapter 8.6), where the inlets of recirculation ducts are located. By recirculating are these hot gases directed close to the axis of the chamber and less heat energy is recovered to the water-cooled shell compared to the case without recirculation. The heat energy is then taken out of the chamber with the flue gases. This is in accordance with the total heat flow rates to the shell (see Fig. 40), since for the recirculating burner with 4.5 mm orifice the lowest heat flow rates to the shell were measured. Likewise, the calculated thermal efficiency was the lowest for this configuration (see chapter 8.5).

At the recirculating burner, temperatures of recirculated flue gas were also measured inside the recirculation duct. The results of these measurements are presented in Fig. 35.

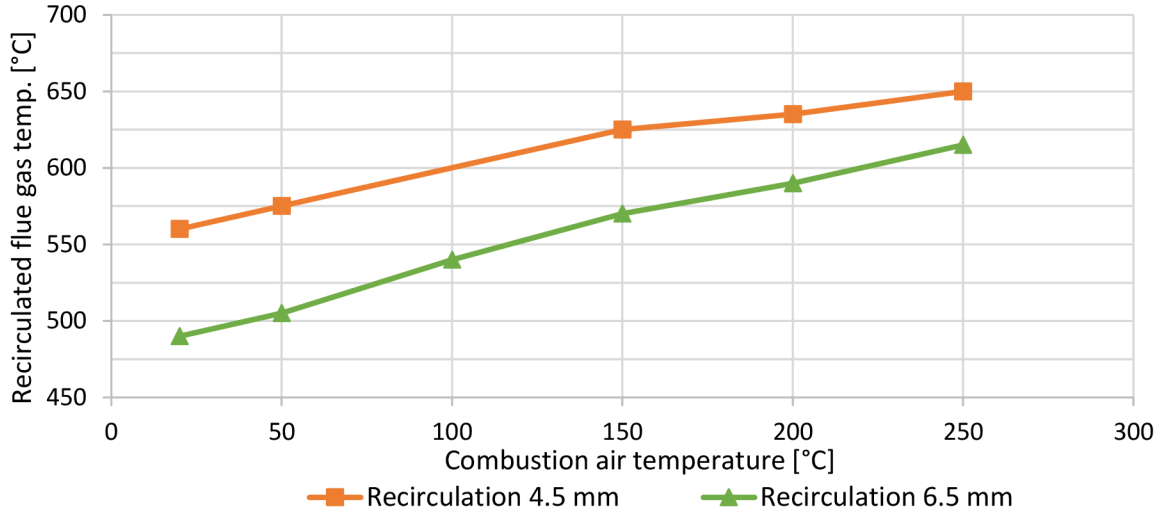


Fig. 35: Dependence of recirculated flue gas temperature on combustion air temperature

Temperatures of the recirculated flue gas were higher with smaller orifice diameter. As already mentioned above, smaller orifice diameter means that more fuel is distributed to the secondary stage which results in higher temperatures close to the wall (as can be seen from temperature profiles shown in chapter 8.6) where the inlets of recirculation ducts are located. With higher combustion temperature, the difference between these two settings was slightly lower. However, this measurement could be burdened with higher uncertainty, because it was not possible to fully ensure that the thermocouple was every time inserted to the same position in the duct. Moreover, it would be necessary to measure the temperatures at more points in each duct in order to obtain more accurate results.

## 8.4 Heat fluxes

Heat fluxes to the shell were calculated from the measured cooling water input and output temperatures. These temperatures were recorded for 14 minutes at a sampling frequency of 2 minutes. In view of the fact that density and specific heat capacity of water are dependent on temperature, it was necessary to calculate values of this quantities using following formulas [52]:

$$\rho = 1006 - 0.26 \cdot \frac{t_{in} + t_{out}}{2} - 0.0022 \cdot \left( \frac{t_{in} + t_{out}}{2} \right)^2 \quad (8.3)$$

$$c_p = 4210 - 1.363 \cdot \frac{t_{in} + t_{out}}{2} + 0.014 \cdot \left( \frac{t_{in} + t_{out}}{2} \right)^2 \quad (8.4)$$

For each section and combustion air temperature, values of both above stated quantities were calculated. The heat flow rate [W] is than given by the following formula:

$$\dot{Q} = \dot{m} \cdot c_p \cdot \Delta t = \rho \cdot \dot{V} \cdot c_p \cdot (t_{out} - t_{in}) \quad (8.5)$$

After dividing the heat flow by the heat transfer area, the heat flux [ $\text{W} \cdot \text{m}^{-2}$ ] for the  $i$ -th section was obtained:

$$\dot{q}_i = \frac{\dot{Q}_i}{A_i} = \frac{\dot{Q}_i}{\pi \cdot d \cdot L_i} \quad (8.6)$$

As soon as a thermodynamic steady state was reached in the chamber (Fig. 36), heat fluxes were recorded. The resulting heat fluxes along the combustion chamber are visualized in Fig. 37 to Fig. 39.

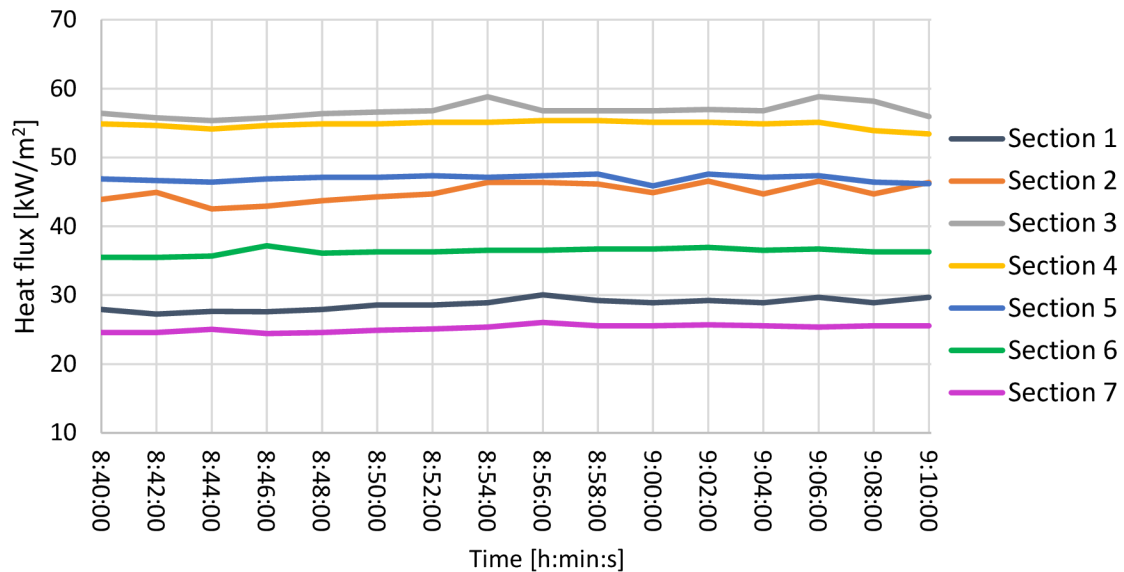


Fig. 36: Example of heat fluxes in a thermodynamic steady state

The obtained shape of the heat flux curves was similar for all investigated settings. In general, the highest heat fluxes were reached in the third section whereas the lowest heat fluxes were achieved in the last seventh section for all three settings. In this section furthest from the burner, the heat fluxes were almost independent on combustion air temperature (ca.  $25 \text{ kW}\cdot\text{m}^{-2}$  for all settings). With higher combustion air temperature, the heat flux is higher owing to a higher amount of heat energy supplied to the combustion chamber. The absolutely highest heat flux (over  $70 \text{ kW}\cdot\text{m}^{-2}$ ) was reached at the recirculating burner with 6.5 mm orifice for combustion air temperature of  $250 \text{ }^\circ\text{C}$ . Difference in heat fluxes between preheated and non-preheated air was highest in the third section for the fuel-staged burner. Using the combustion air at ambient temperature, the heat flux in this section was lower by  $10.2 \text{ kW}\cdot\text{m}^{-2}$  compared to the air preheated to  $250 \text{ }^\circ\text{C}$ . As far as the recirculating burner is concerned, this difference was highest in the second section for both orifice sizes (almost  $16.5 \text{ kW}\cdot\text{m}^{-2}$  for 4.5 mm orifice;  $14.0 \text{ kW}\cdot\text{m}^{-2}$  for 6.5 mm orifice).



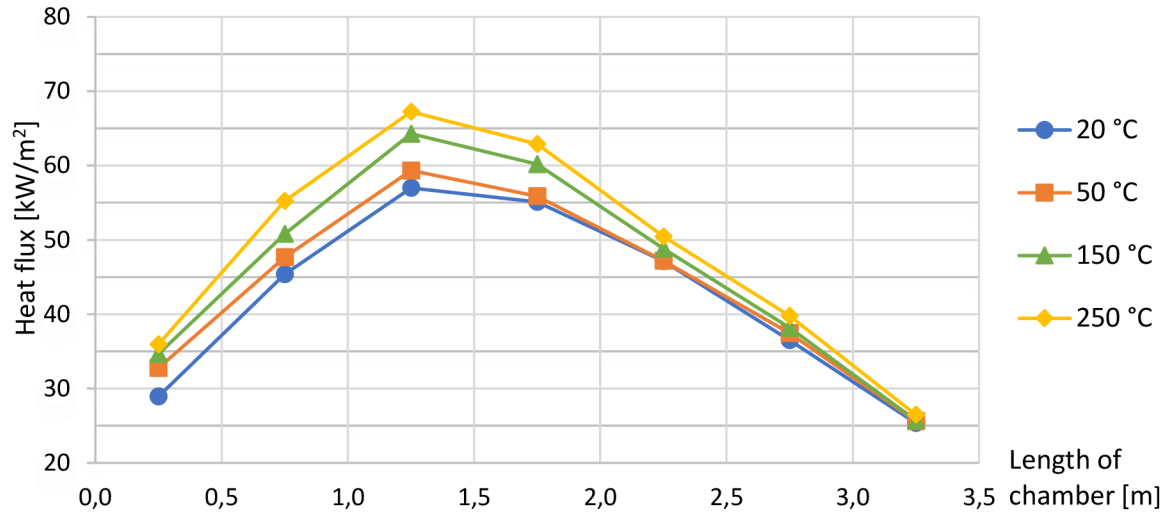


Fig. 37: Fuel-staged burner, 4.5 mm orifice – heat fluxes at different combustion air temperatures

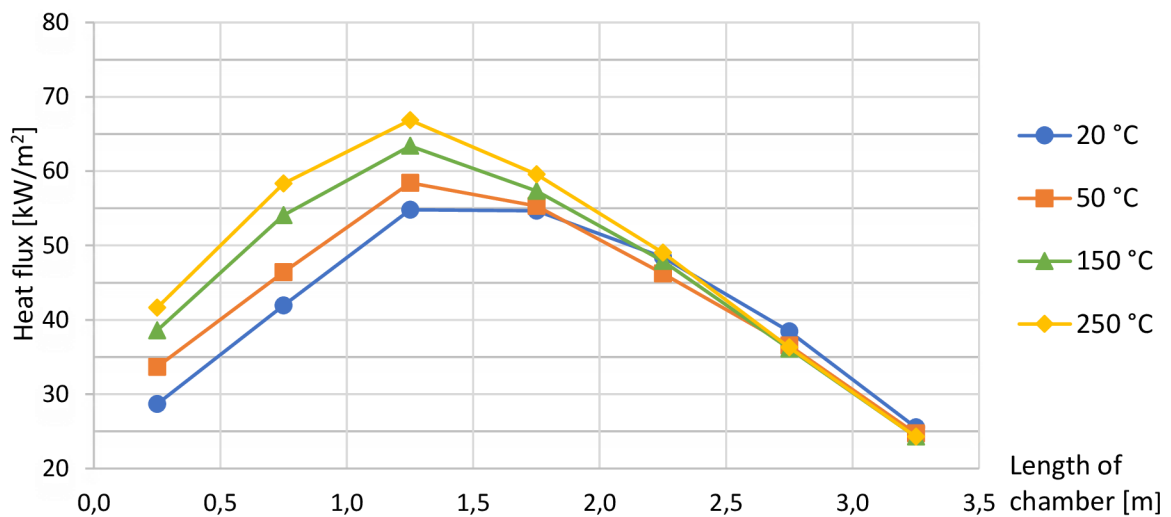


Fig. 38: Recirculating burner, 4.5 mm orifice – heat fluxes at different combustion air temperatures

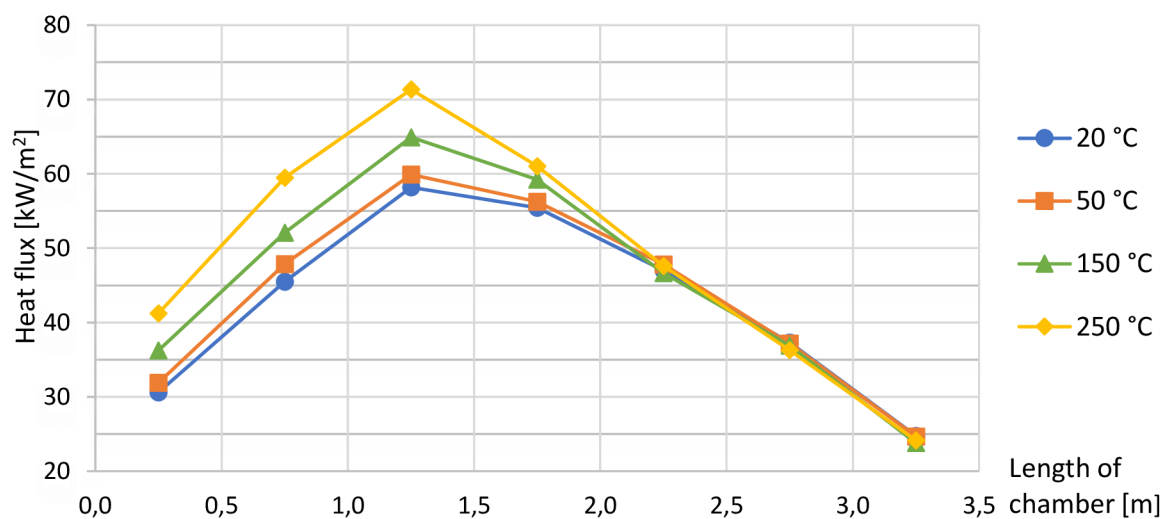


Fig. 39: Recirculating burner, 6.5 mm orifice – heat fluxes at different combustion air temperatures

Similar shapes of the heat flux curves were experimentally obtained at the same testing facility by e.g. Hudák [51], who carried out tests of a fuel-staged burner at higher oxygen concentration. Another investigation was done with a recirculating fuel-staged burner by Macenauerová [49], having the maximum heat fluxes likewise in the third section of the chamber.

For each burner configuration, the total heat flow rates at investigated temperatures were calculated as a sum of heat flow rates in all seven sections ( $i = 1$  to 7):

$$\dot{Q} = \Sigma(q_i \cdot A_i) \quad (8.7)$$

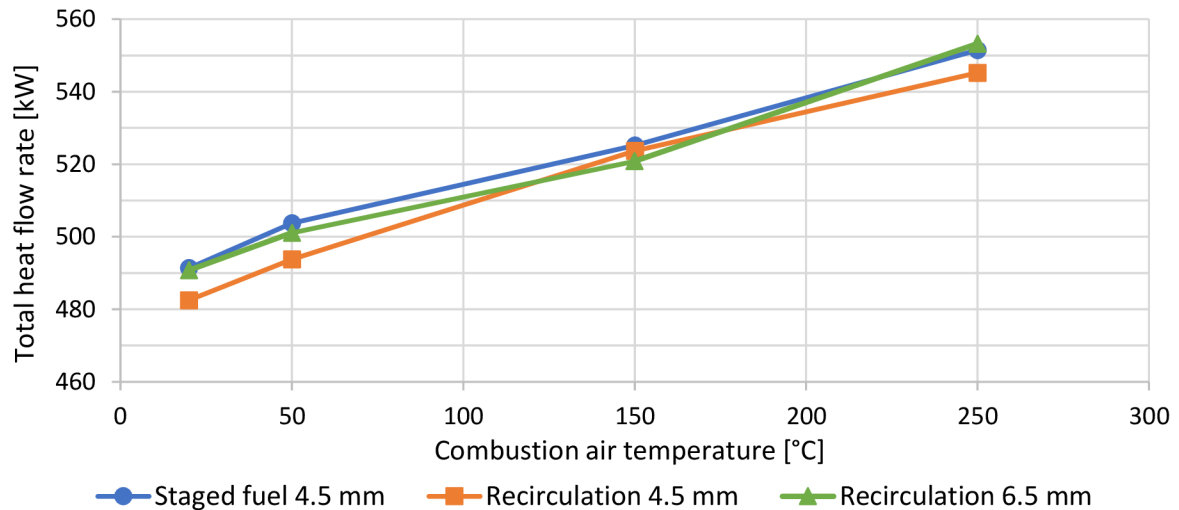


Fig. 40: Influence of combustion air temperature on overall heat flow rate in the combustion chamber

As can be seen in Fig. 40, the values of total heat flow rates in the investigated temperature range increased approximately linear with higher combustion temperature due to higher total heat input to the combustion chamber. At the fuel-staged burner and the recirculating burner with 4.5 mm orifice, the values of heat flow rates were almost identical (ca. 490 kW without air preheating, 550 kW with air preheated to 250 °C). At the recirculating burner with 4.5 mm orifice, the total heat flows were lower by ca. 7 kW (at three of four temperature points), which could be caused by higher amount of heat energy taken out of the chamber by the flue gases (see chapter 8.3), or alternatively by a slightly lower stability of combustion (as discussed in chapter 8.7).

## 8.5 Efficiency of the radiant section

The thermal efficiencies of the radiant section were calculated for all configurations from the heat flow rates. First, the volumetric flow rate of fuel supplied to the burner was calculated according to the formula (8.8) from the known thermal input  $P_H = 750$  kW, which is released by combustion of the fuel:

$$\dot{V}_{fuel} = \frac{P_H}{LHV} \quad (8.8)$$

Information about chemical composition of the natural gas and its lower heating value ( $LHV = 34.615 \text{ MJ} \cdot \text{m}_N^{-3}$ ) are provided by the gas supplier company [53]. Next, based on the required concentration of  $\text{O}_2$  in dry flue gas 3 % vol., the volumetric flow rate of the combustion air was calculated using a simple simulation carried out in ChemCad software.

From the simulation, the values of mass flow rates and specific heat capacities were also ascertained for both air and fuel. The flow rate values are presented in Tab. 8.

Tab. 8: Flow rates of fuel and combustion air obtained from ChemCad simulation

Fuel volumetric flow rate	$\dot{V}_{fuel} = 78 \text{ mN}^3 \cdot \text{h}^{-1}$
Fuel mass flow rate	$\dot{m}_{fuel} = 58 \text{ kg} \cdot \text{h}^{-1}$
Combustion air volumetric flow rate	$\dot{V}_{air} = 867 \text{ mN}^3 \cdot \text{h}^{-1}$
Combustion air mass flow rate	$\dot{m}_{air} = 1116 \text{ kg} \cdot \text{h}^{-1}$

Then, enthalpy flow rates of fuel and combustion air with reference to the standard temperature (273.15 K) were calculated using formula (8.9). The obtained results (Tab. 9) were converted into kW units, which are equal to  $\text{kJ} \cdot \text{s}^{-1}$ .

$$\dot{H} = \dot{m} \cdot c_p \cdot \Delta T \quad (8.9)$$

Tab. 9: Calculated enthalpy flow rates of fuel and combustion air at investigated temperatures

Fuel enthalpy flow rate	20 °C	$\dot{H}_{fuel} = 0.7 \text{ kW}$
Combustion air enthalpy flow rate	20 °C	$\dot{H}_{air\ 20} = 6.3 \text{ kW}$
	50 °C	$\dot{H}_{air\ 50} = 15.7 \text{ kW}$
	150 °C	$\dot{H}_{air\ 150} = 47.6 \text{ kW}$
	250 °C	$\dot{H}_{air\ 250} = 80.7 \text{ kW}$

According to API 560, Appendix G [54], the efficiency of radiant section can be defined as heat absorbed to the water-cooled shell divided by the total heat input to the system. The total heat input can be calculated as a sum of fuel enthalpy flow rate, combustion air enthalpy flow rate and heat flow rate released by combustion of the fuel. Thus, the thermal efficiency [%] was calculated as following:

$$\eta = \frac{\dot{Q}}{\dot{H}_{fuel} + \dot{H}_{air} + P_H} \cdot 100 \quad (8.10)$$

The results are shown in Fig. 41. The efficiency of the radiant section was slightly increasing with the combustion air temperature. This is in accordance with Baukal [31], since the available heat is also increasing with the temperature, as described in chapter 6. The efficiencies are lower for the both settings with recirculation than for the fuel-staged burner. However, the increase of efficiency with combustion air preheating was not very significant, since the enthalpy flow rates of the combustion air (Tab. 9) are minor compared to the 750 kW released by combustion of the fuel. For the fuel-staged burner without recirculation, the efficiency increased from 64.9 % (without preheating) to 66.3 % (preheating to 250 °C), for the recirculating burner with 4.5 mm orifice was an increase from 63.7 to 65.6 % calculated. Nevertheless, even a minor increase in the efficiency may lead to significant savings in industrial applications.

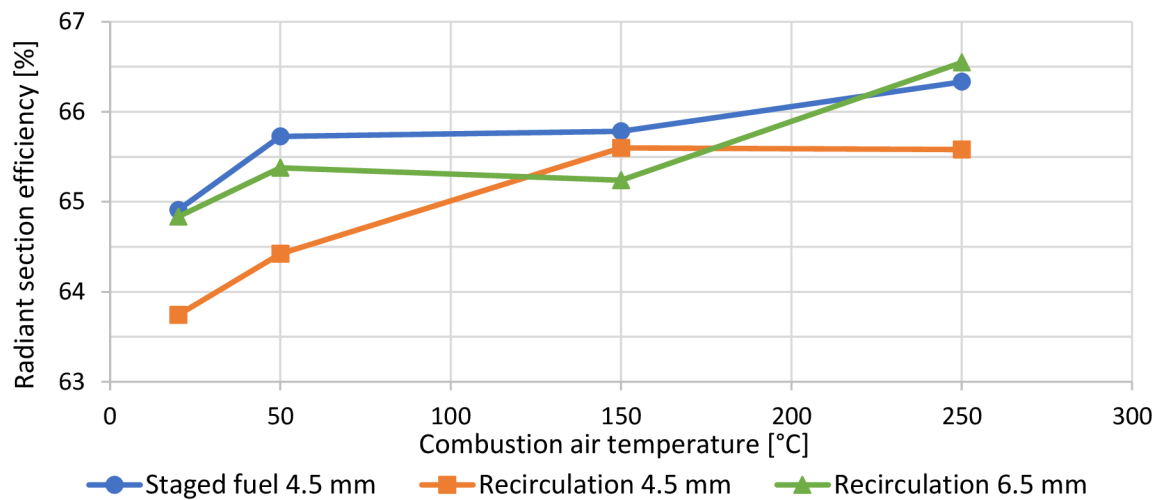


Fig. 41: Influence of combustion air temperature on the radiant section efficiency

As already stated in chapter 8.3, lower efficiency of the recirculating burner could be explained by the fact that hot gases from the surroundings of the secondary fuel nozzles are recirculated to the central area close to the axis of the chamber and less heat energy is transferred to the shell in comparison to the burner without recirculation, because the heat energy is taken out of the chamber with the flue gases.

## 8.6 Temperature distribution

Another aim of the experimental part of this thesis was to investigate the influence of combustion air temperature on temperature distribution in the chamber. The temperatures were measured by R-type thermocouples described in chapter 7.1.3. It was assumed that the temperature distribution is symmetric with respect to a vertical plane passing through the axis of the cylindrical chamber, so the temperatures were measured in one half of the chamber only. As mentioned in chapter 7.1.1, there are eight inspection holes on each side of the chamber. Spacing between these holes is 0.5 m. In each of the eight holes, a thermocouple was placed. It was possible to move the thermocouples in radial direction towards to the chamber axis. The temperatures were measured in distances 5, 10, 20, 30, 40 and 50 cm from the inner shell. Since the inner diameter of the chamber is equal to 1 m, the last position was situated exactly on the axis of the chamber. At each position, the data were collected for a time period of 30 seconds at a sampling frequency of 1 second. Afterwards, an arithmetic mean was evaluated from this data set. For each setting, altogether 48 values were obtained at every investigated combustion air temperature (8 thermocouples, 6 positions).

These values were visualized using a simple script written in Python programming language. The resulting temperature profiles are presented in Fig. 42 to 44. For all settings, the highest temperatures were measured near the axis of the chamber in distance approximately 1.25 m from the burner. Near the walls of the chamber, temperatures were lower compared to the axis because the heat from this area was transferred to the cooled shell. The influence of the combustion air temperature was not very significant for all settings. The peak temperature was roughly 1300 °C. With higher combustion air temperature, the area covered with this peak temperature was slightly larger. The lowest temperatures (circa 650 °C) were recorded by the end of the combustion chamber opposite to the burner.

For the fuel-staged burner, the area with the peak temperature was not as large as for the recirculating burner. In the surroundings of the recirculating burner, higher temperatures were observed when using the orifice with a larger diameter. This was caused by the fact that larger diameter of the orifice results in supplying higher amount of fuel to the primary fuel nozzles, which are located close the axis of the chamber and the supplied heat is concentrated to a smaller area. With smaller diameter of the orifice (4.5 mm), the supplied heat was distributed more uniformly across the width of the chamber (compared to the 6.5 mm orifice) due to higher amount of fuel supplied to secondary stage, which led to the reduction of  $\text{NO}_x$ , as shown in Fig. 32.

In any other plane than the horizontal one, the distribution of temperatures could be slightly different due to combustion air swirling behind the burner. However, this testing facility currently does not allow to measure temperatures inside the chamber in any other planes.

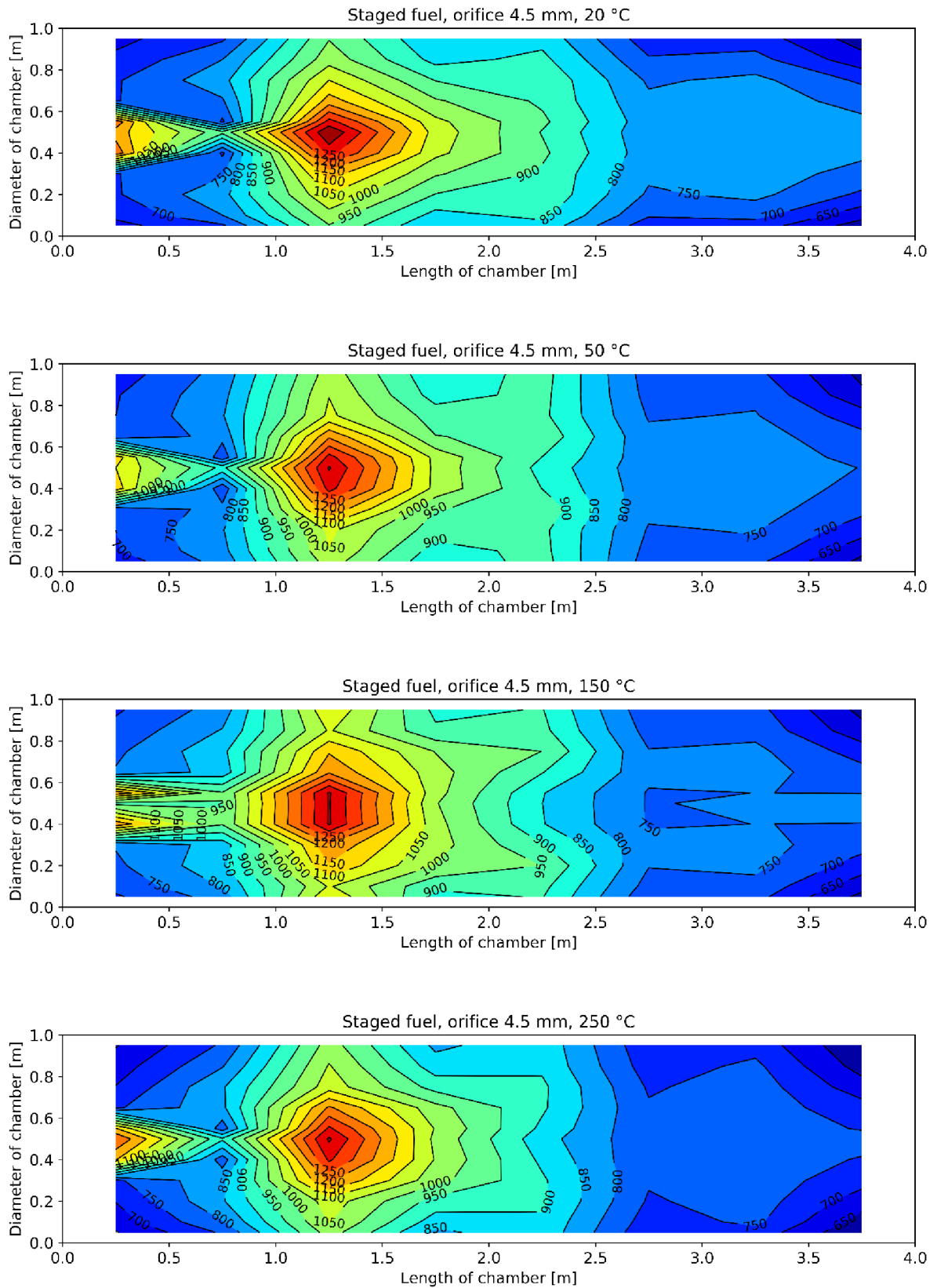


Fig. 42: Fuel-staged burner, 4.5 mm orifice – temperature distribution in the combustion chamber

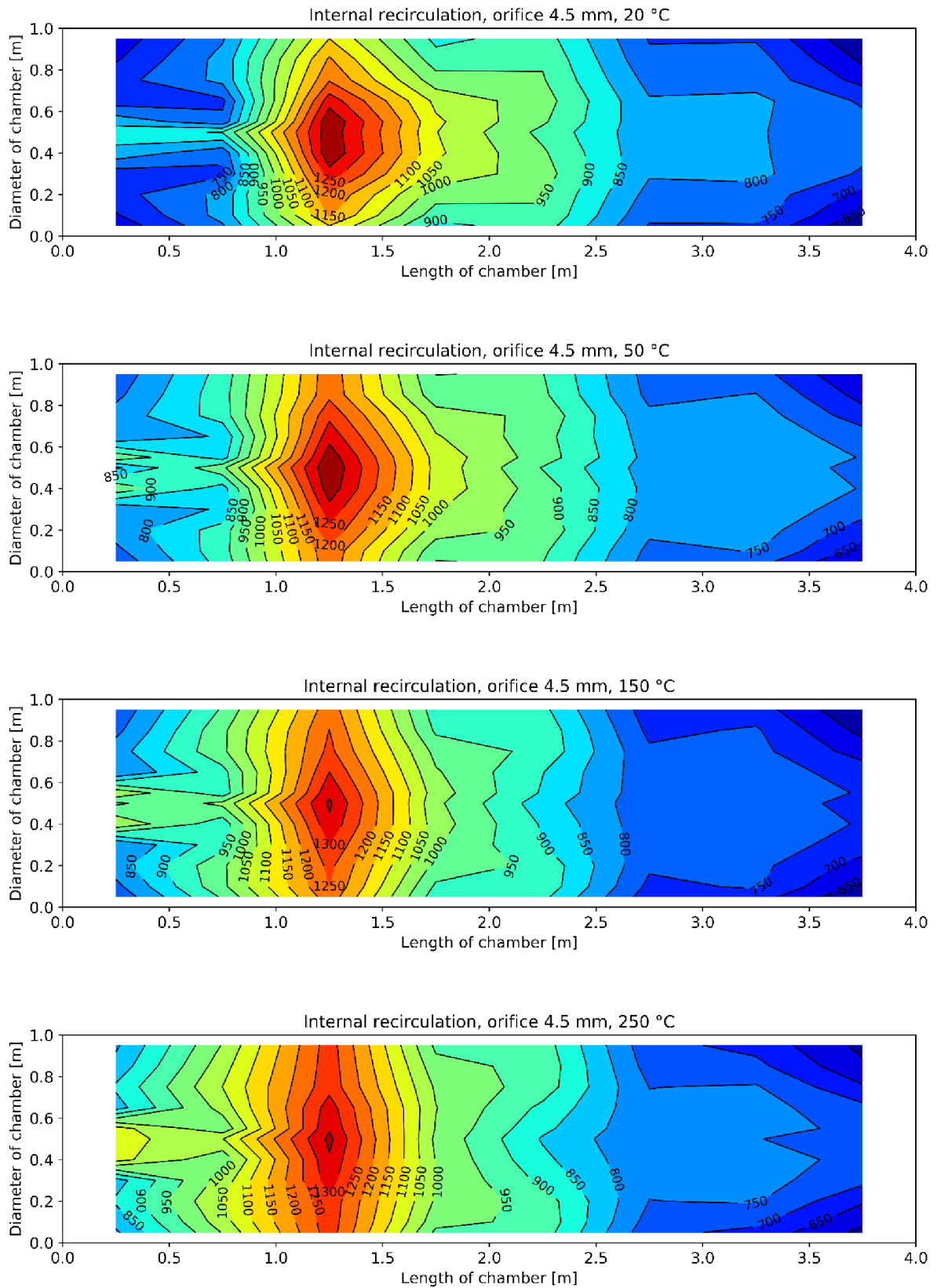


Fig. 43: Recirculating burner, 4.5 mm orifice – temperature distribution in the combustion chamber

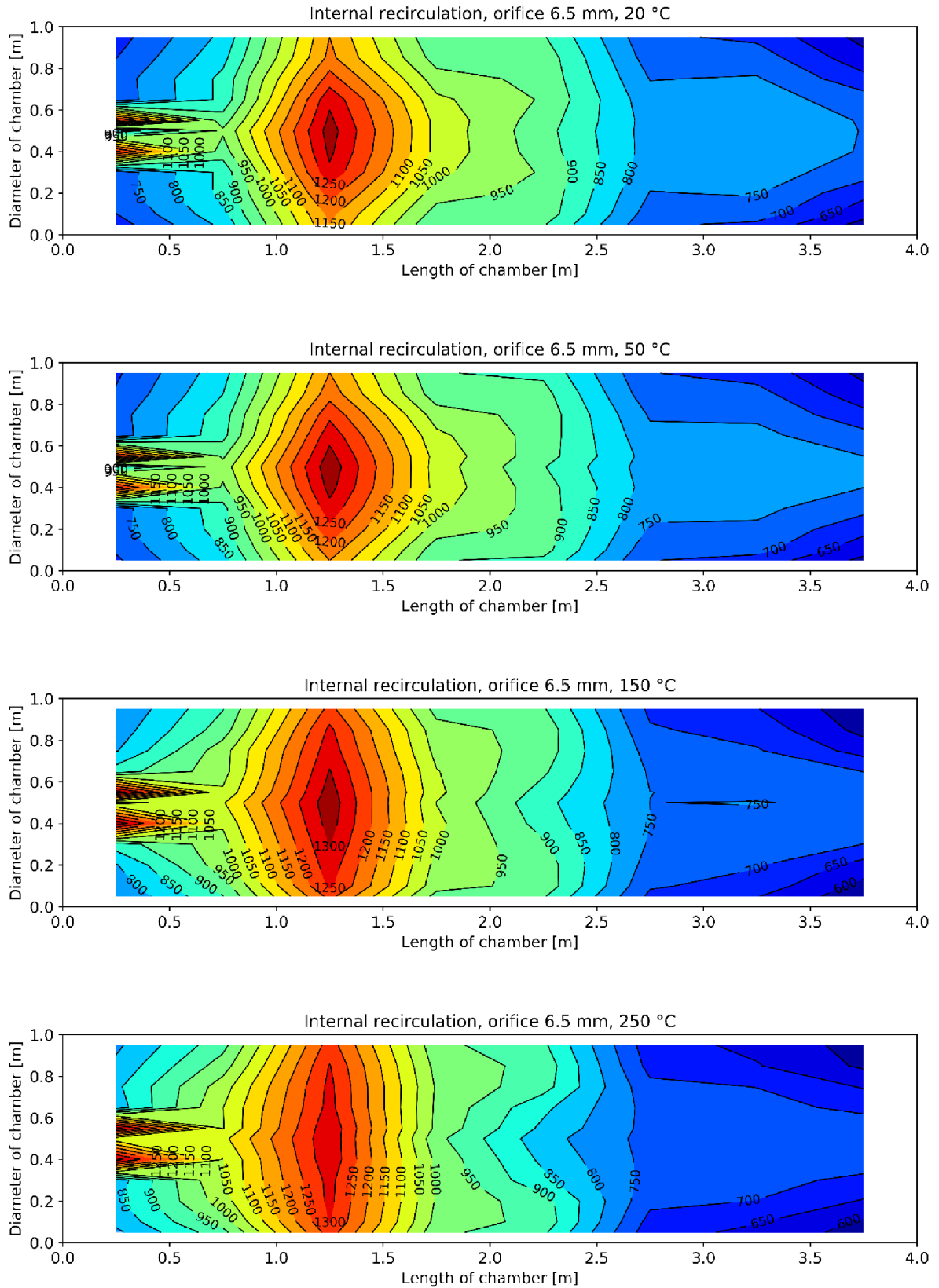


Fig. 44: Recirculating burner, 6.5 mm orifice – temperature distribution in the combustion chamber



## 8.7 Flame stability

At selected temperatures of combustion air (20, 50, 150 and 250 °C), the range of flame stability was investigated as a function of O<sub>2</sub> concentration in the flue gas. The O<sub>2</sub> concentration in the flue gas was controlled by regulating the amount of combustion air fed to the burner. The obtained results are presented in Fig. 45 to Fig. 47.

At the level of 3 % O<sub>2</sub> vol. (on dry basis) in the flue gas, the flames were stable for all three burner configurations. At first, both lower and upper O<sub>2</sub> concentrations in flue gas were found, at which first instabilities (e.g. blow-off at the secondary fuel nozzles, flame pulsation) occurred. Nevertheless, at a low air surplus, the amount of CO emissions exceeded the current valid legislative limit 50 mg·m<sup>-3</sup> due to incomplete combustion. With further decrease of the air surplus, CO emissions increase rapidly up to 1000 mg·m<sup>-3</sup>. As can be seen from the diagrams, the proper operational range of the burners is situated between the 'CO emissions curve' and the 'upper stability curve'. When the air surplus was increased over the upper stability limit, major flame instabilities (e. g. significant blow-off), were observed at certain O<sub>2</sub> concentration even at the primary nozzles due to very lean fuel conditions.

For operating in compliance with the legislative limit 50 mg·m<sup>-3</sup>, the lowest allowable O<sub>2</sub> concentration in the dry flue gas was around 1.4 % vol. for all settings. The influence of combustion air temperature on the operational range was not very significant. The upper limit oxygen concentration in flue gas, at which major instabilities occurred, was increasing with preheating temperature. For the air preheated to 250 °C, the border value was by ca. 1 % O<sub>2</sub> vol. higher (1.5 % for the recirculating burner with 6.5 mm orifice) compared to the case without preheating.

The widest range was obtained for the fuel-staged burner without recirculation, which could be operated without any obvious flame instabilities up to 6.4 % vol. O<sub>2</sub> in the flue gas. On the contrary, the narrowest operational range was obtained for the recirculating burner with 4.5 mm orifice due to higher amount of fuel supplied to the secondary stage (compared to the 6.5 mm orifice), which negatively influenced stability of the primary flame. For this 4.5 mm orifice combined with recirculation, the upper stability limit was found out at approximately 4.5 % O<sub>2</sub>. This was in accordance with the previous experimental investigation carried out by Bělohradský [46], who found out that decreasing the orifice diameter at the recirculating burner led to lower flame stability due to lower amount of fuel supplied to the primary stage.

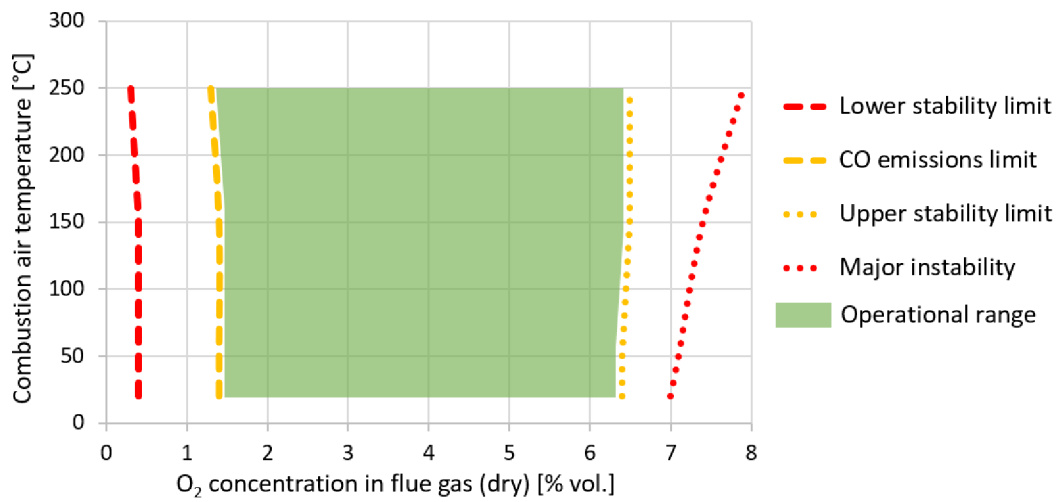


Fig. 45: Fuel-staged burner, 4.5 mm orifice – flame stability diagram

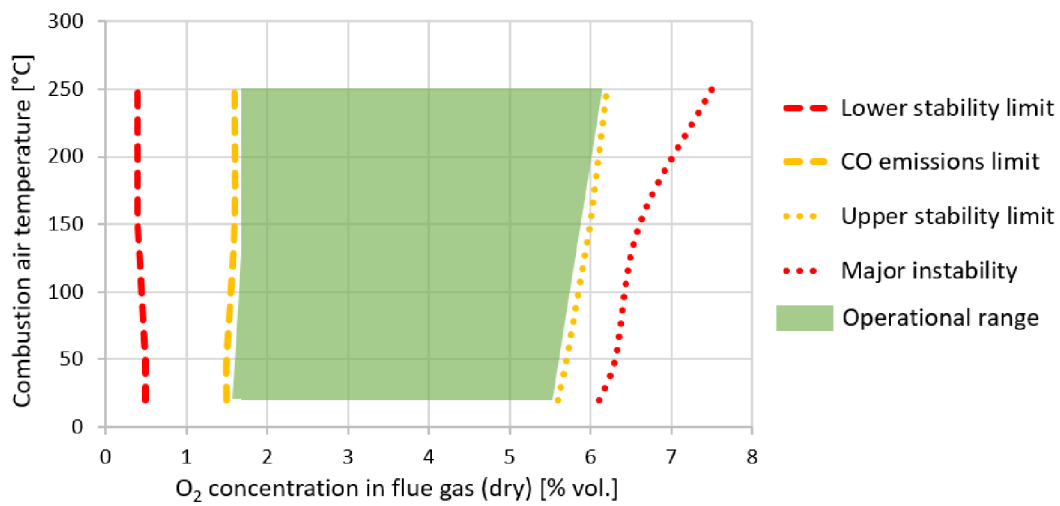


Fig. 46: Recirculating burner, 6.5 mm orifice – flame stability diagram

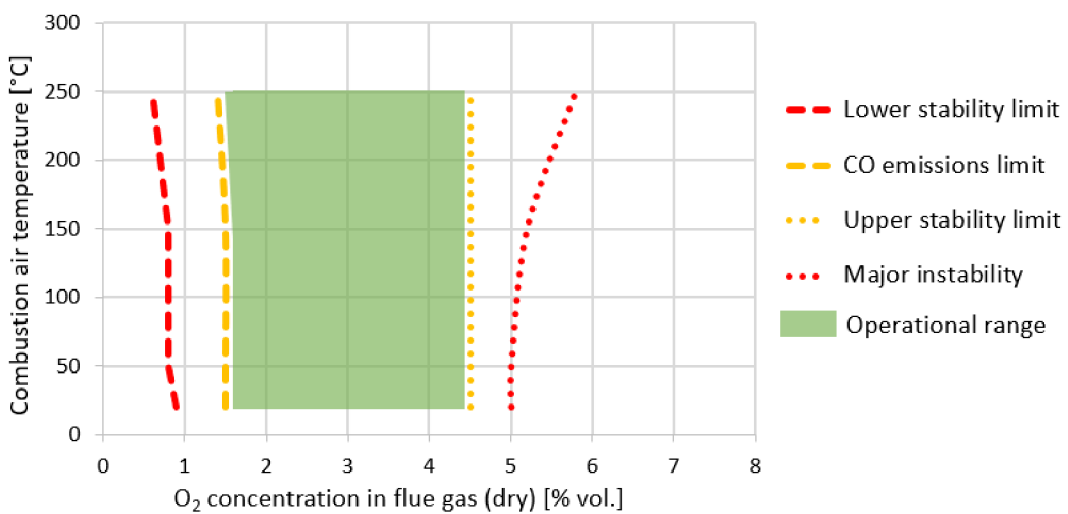


Fig. 47: Recirculating burner, 4.5 mm orifice – flame stability diagram

## 8.8 Flame pattern

Another task of the experimental investigation was to describe the flame pattern. Determination of flame parameters like colour, length and diameter of the visible part was based on subjective observations through the inspection windows.

The results were similar for all three burner configurations. Throughout all tests, the observed flames were sharp and stable at the oxygen concentration 3 % vol. in dry flue gas. Without preheating the combustion air, the flame was characterised by a blue core and a yellow envelope. At higher preheating temperatures was the content of yellow colour increasing.

With increasing combustion air temperature, the length of the flame was decreasing slightly. The length of the flame was ca. 2.8 m without preheating, while at combustion air temperature of 250 °C, the flame was by approximately 0.4 m shorter due to higher oxidation rate of the fuel at higher temperatures. Thus, the fuel needs shorter distance to complete the burnout compared to the case with non-preheated air.

The diameter of the flame was independent on the combustion air temperature. For the settings with a 4.5 mm orifice, the diameter was equal to ca. 0.9 m. For the recirculating burner with a 6.5 mm orifice, the diameter was by 0.1–0.2 m lower due to smaller amount of fuel supplied to the secondary fuel nozzles, which are located closer to the wall than the primary fuel nozzles (see chapter 7.2)

These results are in accordance with the results experimentally obtained by Gupta et al. [43], who proved by emission spectroscopy that the increased flame luminosity at higher preheating temperatures was caused by higher concentrations of  $\bullet\text{OH}$ ,  $\text{CH}\bullet$ , and  $\text{C}_2$ , which cause the radiation in the visible spectrum.

## 9 Conclusions

In the first part of this master's thesis, a classification of industrial burners according to different criteria was carried out, including mixing type, draft type, fuel type and concentration of oxygen in the oxidizer. Some pollutants from combustion processes ( $\text{CO}$ ,  $\text{NO}_x$ ) can be reduced by changing the conditions and burner setting, however, abatement of some pollutants ( $\text{SO}_x$ ) requires a post-combustion treatment. For the combustion processes, radiation is the most important mechanism of heat transfer, as described in chapter 4.

The legislative measures concerning emissions from industrial combustion are in the EU member countries based on the directives of the European Parliament. However, the way of implementation of these directives into national legislations is at the countries' decision. The emission limits for pollutants may thus differ in the particular member countries. However, these limit values must not be higher than the limit values given by the EU legislation. The information about releases of pollutants can be found in the European Pollutant Release and Transfer Register as well as in the national registers.

In the experimental part, an investigation with combustion air preheated up to  $250\text{ }^\circ\text{C}$  was carried out at a large-scale burner testing facility. During all the tests, natural gas was used as fuel. The thermal input to the burner was constantly equal to  $750\text{ kW}$ . It was possible to increase the ratio of fuel supplied into the primary stage by increasing diameter of the exchangeable orifice at primary fuel inlet. The concentration of oxygen in flue gas was maintained constantly at  $3\%$  vol. by regulating the volume flow of the combustion air. The following three burner configurations were investigated:

- Fuel-staged diffusion burner, orifice diameter  $4.5\text{ mm}$
- Fuel-staged diffusion burner with internal recirculation, orifice diameter  $4.5\text{ mm}$
- Fuel-staged diffusion burner with internal recirculation, orifice diameter  $6.5\text{ mm}$

The investigated parameters of the combustion process included:

- $\text{NO}_x$  and  $\text{CO}$  emissions
- Flue gas temperature
- Heat fluxes to the water-cooled shell
- Thermal efficiency of the radiant section
- Temperature distribution across the combustion chamber
- Flame pattern and stability

Higher combustion air temperature led within the investigated temperature range to a nearly linear increase of the measured  $\text{NO}_x$  concentration in the flue gas due to increased formation of  $\text{NO}_x$  via the thermal mechanism. At combustion air temperatures above  $150\text{ }^\circ\text{C}$ , the valid legislative limit of  $\text{NO}_x$   $100\text{ mg}\cdot\text{m}_N^{-3}$  was exceeded for two out of the three burner configurations. The very low amount of carbon monoxide emissions ( $0$  to  $3\text{ mg}\cdot\text{m}_N^{-3}$ ) indicated a nearly complete combustion.

The temperature of the flue gas was increasing with the combustion air temperature. Nevertheless, this increase was not very significant, since the difference in flue gas temperature between the case without preheating and the one with air preheated to  $250\text{ }^\circ\text{C}$  was not higher than  $20\text{ }^\circ\text{C}$ . The explanation is that the enthalpy of the combustion air is minor in comparison to the heat energy released by combustion of the fuel.

Further, heat fluxes to the shell were measured indirectly, based on the increase in cooling water temperature. The highest heat fluxes were obtained in the third section from the burner.

Preheating the combustion air to 250 °C led to an increase in the total heat flow rate to the shell by approximately 60 kW and to efficiency of the radiant section by ca. 1.7 % higher compared to the non-preheated air due to higher available heat in the system. Nevertheless, even a minor increase in efficiency can bring large financial savings in industrial applications.

Based on subjective observations, flame pattern and stability were evaluated. At oxygen level of 3 % vol. in dry flue gas, the flame was stable within the entire temperature range. The widest stable operational range as a function of air surplus was noticed for the fuel-staged burner without recirculation. In general, the influence of combustion air preheating on stability of the combustion process was not significant. However, at even higher combustion air temperatures than used in this investigation, lower stability would be expected due to higher volumetric flow rates of the air according to the equation of state. Without combustion air preheating, a blue core and a yellow envelope of the flame were observed. With increasing combustion air temperature, the flame luminosity as well as the content of yellow colour were increasing. A shorter flame was observed at higher temperatures due to higher rate of fuel oxidation.

In industrial applications, waste heat is often utilized for preheating the combustion air, which can result to fuel savings and thus to reduction of carbon dioxide emissions produced by combustion of fossil fuels. During the carried out experimental investigation, an auxiliary burner was used for the preheating in order to ensure an easier control of the combustion air temperature. A contradiction between efficiency and economy on the one hand and amount of pollutant emissions on the other hand may occur in many combustion processes. Thus, a thoroughgoing analysis is always necessary for each particular case in order to optimize the process parameters. For a detailed description of flow patterns in the combustion chamber and obtaining more accurate results within the scope of this thesis, it would be necessary to carry out a CFD investigation. This could be subject of another final thesis in the future.

## List of symbols

$A$	$[\text{m}^2]$	area
$c_p$	$[\text{J}\cdot\text{kg}^{-1}\cdot\text{K}^{-1}]$	specific heat capacity at constant pressure
$d$	$[\text{m}]$	inner diameter of the combustion chamber
$\dot{H}$	$[\text{W}]$	enthalpy flow rate
$L$	$[\text{m}]$	characteristic dimension
$L_i$	$[\text{m}]$	length of $i$ -th section of the combustion chamber
$LHV$	$[\text{J}\cdot\text{m}^{-3}]$	lower heating value
$M$	$[\text{kg}\cdot\text{mol}^{-1}]$	molecular mass
$\dot{m}$	$[\text{kg}\cdot\text{s}^{-1}]$	mass flow rate
$Nu$	$[-]$	Nusselt number
$T$	$[\text{K}]$	thermodynamic temperature
$t$	$[\text{°C}]$	temperature
$p$	$[\text{Pa}]$	pressure
$P_H$	$[\text{W}]$	thermal input to the burner from combustion of the fuel
$Pr$	$[-]$	Prandtl number
$\dot{Q}$	$[\text{W}]$	heat flow rate
$\dot{q}$	$[\text{W}\cdot\text{m}^{-2}]$	heat flux
$Re$	$[-]$	Reynolds number
$u$	$[\text{m}\cdot\text{s}^{-1}]$	flow velocity
$V_M$	$[\text{m}^3\cdot\text{mol}^{-1}]$	molar volume
$\dot{V}$	$[\text{m}^3\cdot\text{s}^{-1}]$	volumetric flow rate
$x$	$[\text{m}]$	length coordinate
$\alpha$	$[\text{W}\cdot\text{m}^{-2}\cdot\text{K}^{-1}]$	heat transfer coefficient
$\varepsilon$	$[-]$	emissivity
$\lambda$	$[\text{W}\cdot\text{m}^{-1}\cdot\text{K}^{-1}]$	thermal conductivity
$\nu$	$[\text{m}^2\cdot\text{s}^{-1}]$	kinematic viscosity
$\rho$	$[\text{kg}\cdot\text{m}^{-3}]$	density
$\sigma$	$[\text{W}\cdot\text{m}^{-2}\cdot\text{K}^{-4}]$	Stefan–Boltzmann constant
$\eta$	$[\%]$	combustion efficiency

## List of chemical formulas

$C_2$	diatomic carbon
$CaSO_4$	calcium sulphate
$CO$	carbon monoxide
$CO_2$	carbon dioxide
$CH\bullet$	methylidene radical
$C_xH_y$	hydrocarbon (in general)
$H_2SO_3$	sulphurous acid
$H_2SO_4$	sulphuric acid
$HCN$	hydrogen cyanide
$HNO_3$	nitric acid
$N_2$	molecular nitrogen
$NH_3$	ammonia
$NO$	nitrogen monoxide
$NO_2$	nitrogen dioxide
$NO_x$	nitrogen oxides (monoxide and dioxide)
$O_2$	molecular oxygen
$\bullet OH$	hydroxyl radical
$SO_2$	sulphur dioxide
$SO_3$	sulphur trioxide
$SO_x$	sulphur oxides (dioxide and trioxide)

## List of abbreviations

API	American Petroleum Institute
BImSchG	Bundes-Immissionsschutzgesetz
BImSchV	Bundes-Immissionsschutzverordnung
CENIA	Česká informační agentura životního prostředí
CFD	Computational fluid dynamics
ČHMÚ	Český hydrometeorologický ústav
EC	European Commission
EPER	European Pollutant Emission Register
E-PRTR	European Pollutant Release and Transfer Register

EU	European Union
FGD	Flue gas desulphurization
HiTAC	High Temperature Air Combustion
IRZ	Integrovaný registr znečišťování
MILD	Moderate or Intense Low-oxygen Dilution
NMVOC	Non-methane volatile organic compounds
TA Luft	Technische Anleitung zur Reinhaltung der Luft
UBA	Umweltbundesamt
VOC	Volatile organic compounds

## List of figures

Fig. 1: Primary energy supply worldwide in exajoules between 1971 and 2016 .....	10
Fig. 2: Average monthly CO <sub>2</sub> concentrations in the atmosphere, depicted by the Keeling curve .....	14
Fig. 3: Carbon monoxide emissions as a function of equivalence ratio for two different fuels .....	15
Fig. 4: Average yearly concentration of NO <sub>x</sub> in the Czech Republic, 2017 .....	20
Fig. 5: Comparison of average yearly concentrations of NO <sub>x</sub> in Germany in years 1990 and 2015 .....	24
Fig. 6: Schematic of a diffusion burner .....	27
Fig. 7: Schematic of a premix burner .....	27
Fig. 8: Schematic of a partially premixed burner .....	27
Fig. 9: Schematic of an oxygen-enriched air/fuel burner .....	29
Fig. 10: Schematic of an oxy-fuel burner .....	30
Fig. 11: Adiabatic flame temperature as a function of air preheat temperature for different fuels .....	31
Fig. 12: Available heat as a function of air preheat temperature for different fuels .....	31
Fig. 13: Adiabatic equilibrium of NO emissions as a function of air preheat temperature for stoichiometric air/fuel flames .....	32
Fig. 14: Adiabatic equilibrium of CO emissions as a function of air preheat temperature for stoichiometric air/fuel flames .....	32
Fig. 15: Schematic diagram of the regenerative burner system .....	34
Fig. 16: Predicted fuel consumption improvement by combustion air preheating .....	34
Fig. 17: Temperatures at three different locations in the chamber as a function of combustion air temperature .....	35
Fig. 18: CO and NO <sub>x</sub> emissions as a function of combustion air temperature .....	35
Fig. 19: NO <sub>x</sub> and CO emissions at different combustion air temperatures as functions of equivalence ratio .....	36



---

Fig. 20: Burner testing facility at Institute of Process Engineering .....	37
Fig. 21: Simplified block diagram of the burner testing facility.....	37
Fig. 22: Schematic of the helix and of the water flow in one section.....	38
Fig. 23: View of the jacketed combustion chamber for air preheating.....	39
Fig. 24: Longitudinal and transversal cross-sections of the convection block .....	39
Fig. 25: User interface of the burner testing facility .....	40
Fig. 26: Detail of thermocouples for measuring temperatures in the combustion chamber .....	40
Fig. 27: 3D model of the exchangeable orifice for regulating fuel supply to the primary stage.....	41
Fig. 28: 3D model of the fuel-staged burner .....	41
Fig. 29: Side view of the fuel-staged burner.....	41
Fig. 30: 3D model of the fuel-staged burner with internal recirculation .....	42
Fig. 31: Side view of the fuel-staged burner with internal recirculation .....	42
Fig. 32: Dependence of NO <sub>x</sub> concentrations in the flue gas on combustion air temperature.....	44
Fig. 33: Dependence of CO concentrations in the flue gas on combustion air temperature.....	45
Fig. 34: Dependence of flue gas temperature on combustion air temperature .....	46
Fig. 35: Dependence of recirculated flue gas temperature on combustion air temperature.....	47
Fig. 36: Example of heat fluxes in a thermodynamic steady state .....	48
Fig. 37: Fuel-staged burner, 4.5 mm orifice – heat fluxes at different combustion air temperatures .....	49
Fig. 38: Recirculating burner, 4.5 mm orifice – heat fluxes at different combustion air temperatures .....	49
Fig. 39: Recirculating burner, 6.5 mm orifice – heat fluxes at different combustion air temperatures .....	49
Fig. 40: Influence of combustion air temperature on overall heat flow rate in the combustion chamber.....	50
Fig. 41: Influence of combustion air temperature on the radiant section efficiency .....	52
Fig. 42: Fuel-staged burner, 4.5 mm orifice – temperature distribution in the combustion chamber.....	54
Fig. 43: Recirculating burner, 4.5 mm orifice – temperature distribution in the combustion chamber.....	55
Fig. 44: Recirculating burner, 6.5 mm orifice – temperature distribution in the combustion chamber.....	56
Fig. 45: Fuel-staged burner, 4.5 mm orifice – flame stability diagram .....	58
Fig. 46: Recirculating burner, 6.5 mm orifice – flame stability diagram .....	58
Fig. 47: Recirculating burner, 4.5 mm orifice – flame stability diagram .....	58

---

## List of tables

Tab. 1: Specific emission limits for stationary sources with rated thermal input lower than or equal to 300 kW valid in the Czech Republic from 1.1.2018 .....	18
Tab. 2: Specific emission limits valid in the Czech Republic from 20.12.2018 up to 31.12.2024 for stationary sources with rated thermal input greater than 0.3 MW and lower than 50 MW, excluding piston combustion engines and gas turbines .....	19
Tab. 3: Specific emission limits valid in the Czech Republic for stationary sources with rated thermal input 50 MW or greater, for which a complete application for a permit has been submitted on 7.1.2013 or later, or were put into operation after 7.1.2014.....	19
Tab. 4: The top five NO <sub>x</sub> emissions producers in the Czech Republic, 2017 .....	20
Tab. 5: Emission limits for installations with thermal input greater than 50 MW valid in Germany .....	22
Tab. 6: Emission limits for installations with thermal input lower than 50 MW valid in Germany .....	23
Tab. 7: The top five NO <sub>x</sub> emissions producers in Germany, 2016.....	23
Tab. 8: Flow rates of fuel and combustion air obtained from ChemCad simulation.....	51
Tab. 9: Calculated enthalpy flow rates of fuel and combustion air at investigated temperatures .....	51

## References

- [1] Key World Energy Statistics. In: *International Energy Agency*. [online]. Retrieved 2019-04-30. Available from: <https://www.iea.org/Statistics/kwes/supply>
- [2] UK coal plants must close by 2025, Amber Rudd announces. In: *The Telegraph*. [online]. Retrieved 2019-04-30. Available from: <https://www.telegraph.co.uk/finance/newsbysector/energy/12001752/UK-coal-plants-must-close-by-2025-Amber-Rudd-to-announce.html>
- [3] Germany to phase out coal by 2038 in move away from fossil fuels. In: *Reuters*. [online]. Retrieved 2019-05-01. Available from: <https://www.reuters.com/article/us-germany-energy-coal/germany-to-phase-out-coal-by-2038-in-move-away-from-fossil-fuels-idUSKCN1PK04L>
- [4] Kohleausstieg: Kommission "Wachstum, Strukturwandel und Beschäftigung". In: *Bundesministerium für Umwelt, Naturschutz und nukleare Sicherheit*. [online]. Retrieved 2019-05-01. Available from: <https://www.bmu.de/themen/klima-energie/klimaschutz/kommission-wachstum-strukturwandel-und-beschaeftigung>
- [5] BAUKAL, Charles E., Jr. *The John Zink Hamworthy Combustion Handbook*. 2<sup>nd</sup> ed., Boca Raton: CRC Press, 2013, 1184 p. ISBN 978-1-4398-3961-4
- [6] BAUKAL, Charles E., Jr. *Industrial Combustion Pollution and Control*. New York: M. Dekker, 2004, 904 p. ISBN 978-8247-4694-5.
- [7] SARKAR, Dipak K. *Thermal Power Plant: Design and Operation*. Elsevier, 2015, 1<sup>st</sup> ed., 612 p. ISBN 978-0-12-801575-9.

- 
- [8] MILLER, Bruce G. *Fossil Fuel Emission Control Technologies: Stationary Heat and Power Systems*. Waltham, MA: Elsevier, 2015. 514 p. ISBN 978-01-2801-566-7.
- [9] SKALSKA, Kinga et al. Trends in NO<sub>x</sub> abatement: a review. *Science of the Total Environment*. 2010, Vol. 408, pp. 3976–3989. ISSN 0048-9697.
- [10] ŠIMEČEK, Radek. *Způsoby snižování emisí oxidů dusíku*. Brno: Vysoké učení technické v Brně, Fakulta strojního inženýrství, 2017. 51 p. Supervisor of the bachelor's thesis: Ing. Petr Bělohradský, Ph.D.
- [11] Keeling Curve Lessons. In: *Scripps CO<sub>2</sub> Program*. [online]. Retrieved 2019-04-09. Available from: [http://scrippsco2.ucsd.edu/history\\_legacy/keeling\\_curve\\_lessons](http://scrippsco2.ucsd.edu/history_legacy/keeling_curve_lessons)
- [12] MODAK, Arindam; JANA, Subhra. Advancement in porous adsorbents for post-combustion CO<sub>2</sub> capture. *Microporous and Mesoporous Materials*. 2019, Vol. 276, pp. 107–132. ISSN 1387-1811.
- [13] MOBINI, Sajad et al. Supported Mn catalysts and the role of different supports in the catalytic oxidation of carbon monoxide. *Chemical Engineering Science*. 2019, Vol. 197, pp. 37–51. ISSN 0009-2509.
- [14] LANGLET, David; MAHMOUDI, Said. *EU Environmental Law and Policy*. Oxford: Oxford University Press, 2016. ISBN 978-0-19-875392-6.
- [15] Directive 2001/81/EC of the European Parliament and of the Council on national emission ceilings for certain atmospheric pollutants. Retrieved 2019-02-27. Also available from: <https://eur-lex.europa.eu/legal-content/EN/TXT/?uri=celex%3A32001L0081>
- [16] Regulation 166/2006/EC of the European Parliament and of the Council concerning the establishment of a European Pollutant Release and Transfer Register and amending Council Directives 91/689/EEC and 96/61/EC. Retrieved 2019-02-27. Also available from: <https://eur-lex.europa.eu/legal-content/EN/TXT/?uri=celex:32006R0166>
- [17] Zákon č. 201/2012 Sb., o ochraně ovzduší. Retrieved 2019-03-01. Also available from: <https://www.zakonyprolidi.cz/cs/2012-201>
- [18] Vyhláška č. 415/2012 Sb., o přípustné úrovni znečištění a jejím zjišťování a o provedení některých dalších ustanovení zákona o ochraně ovzduší. Retrieved 2019-03-01. Also available from: <https://www.zakonyprolidi.cz/cs/2012-415>
- [19] Otázky a odpovědi. In: *Integrovaný registr znečištění* [online]. Retrieved 2019-03-09. Available from: <https://www.irz.cz/node/196>
- [20] Vyhledávání úniků a přenosů látek. In: *Integrovaný registr znečištění* [online]. Retrieved 2019-03-10. Available from: <https://portal.cenia.cz/irz/>
- [21] Grafická ročenka 2017. In: *Český hydrometeorologický ústav*. [online]. Retrieved 2019-03-18. Available from: [portal.chmi.cz/files/portal/docs/uoco/isko/grafroc/17groc/gr17cz/Obsah\\_CZ.html](http://portal.chmi.cz/files/portal/docs/uoco/isko/grafroc/17groc/gr17cz/Obsah_CZ.html)
- [22] Gesetz zum Schutz vor schädlichen Umwelteinwirkungen durch Luftverunreinigungen, Geräusche, Erschütterungen und ähnliche Vorgänge. Retrieved 2019-03-14. Also available from: <https://www.gesetze-im-internet.de/bimschg/>
-

- [23] Dreizehnte Verordnung zur Durchführung des Bundes-Immissionsschutzgesetzes. Retrieved 2019-03-15. Also available from: [http://www.gesetze-im-internet.de/bimschv\\_13\\_2013](http://www.gesetze-im-internet.de/bimschv_13_2013)
- [24] Erste Allgemeine Verwaltungsvorschrift zum Bundes-Immissionsschutzgesetz: Technische Anleitung zur Reinhaltung der Luft. Retrieved 2019-03-01. Also available from: <https://www.bmu.de/gesetz/erste-allgemeine-verwaltungsvorschrift-zum-bundes-immissionsschutzgesetz/>
- [25] Entwurf zur Neufassung der Ersten Allgemeinen Verwaltungsvorschrift zum Bundes-Immissionsschutzgesetz. In: *Bundesministerium für Umwelt, Naturschutz und nukleare Sicherheit*. [online]. Retrieved 2019-03-25. Available from: <https://www.bmu.de/gesetz/entwurf-zur-neufassung-der-ersten-allgemeinen-verwaltungsvorschrift-zum-bundes-immissionsschutzgesetz/>
- [26] Emissions-grenzwerte für mittel-große Feuerungs-anlagen gebilligt. In: *Deutscher Bundestag*. [online]. Retrieved 2019-03-25. Available from: <https://www.bundestag.de/dokumente/textarchiv/2018/kw42-de-feuerungsanlagen-573280>
- [27] Question / Answer. In: *Thru.de*. [online]. Retrieved 2019-03-09. Available from: <https://www.thru.de/3/information/questionanswer/>
- [28] Search – PRTR. In: *Thru.de*. [online]. Retrieved 2019-03-09. Available from: <https://www.thru.de/search/?L=3>
- [29] Deutschland-Karten zu Luftschadstoff-Daten. In: *Das Umweltbundesamt*. [online]. Retrieved 2019-03-11. Available from: <https://www.umweltbundesamt.de/deutschland-karten-zu-luftschadstoff-daten>
- [30] PAVELEK, Milan et al. *Termomechanika*. 1<sup>st</sup> ed., Brno: Akademické nakladatelství CERM, 2011, 192 p. ISBN 978-80-214-4300-6.
- [31] BAUKAL, Charles E., Jr. *Industrial Burners Handbook*. Boca Raton: CRC Press, 2004, 808 p. ISBN 978-0-8493-1386-8.
- [32] LIU, Cunxi et al. Experimental investigations of spray generated by a pressure swirl atomizer. *Journal of the Energy Institute*. 2019, Vol. 92, Issue 2, pp. 210–221. ISSN 1743-9671.
- [33] LIU, Changchun et al. Influence of type of burner on NO emissions for pulverized coal preheating method. *Applied Thermal Engineering*. 2015, Vol. 85, pp. 278–286. ISSN 1359-4311.
- [34] BAUKAL, Charles E., Jr. *Oxygen-Enhanced Combustion*. 2<sup>nd</sup> ed., Boca Raton: CRC Press, 2004, 792 p. ISBN 978-1-4398-6228-5.
- [35] BĚLOHRADSKÝ, Petr; SKRYJA, Pavel; HUDÁK, Igor. Experimental study on the influence of oxygen content in the combustion air on the combustion characteristics. *Energy*. 2014, Vol. 75, pp. 116–126. ISSN 0360-5442.
- [36] WU, Kuo-Kuang et al. High-efficiency combustion of natural gas with 21–30% oxygen-enriched air. *Fuel*. 2010, Vol. 89, Issue 9, pp. 2455–2462. ISSN 0016-2361.
- [37] API Recommended Practice 535: Burners for Fired Heaters in General Refinery Services. 3<sup>rd</sup> ed., American Petroleum Institute, 2014. 84 p.

- [38] HAZLEHURST, John. *Tolley's Industrial and Commercial Gas Installation Practice*. 5<sup>th</sup> ed., Oxford: Elsevier, 2009, 592 p. ISBN 978-1-85617-672-9.
- [39] RAFIDI, Nabil; BLASIAK, Włodzimierz. Heat transfer characteristics of HiTAC heating furnace using regenerative burners. *Applied Thermal Engineering*. 2006, Vol. 26, s. 2027-2034. ISSN 1359-4311.
- [40] SUZUKAWA, Yutaka et al. Heat transfer improvement and NO<sub>x</sub> reduction by highly preheated air combustion. *Energy Conversion and Management*. 1997, Vol. 38, Issue 10–13, pp. 1061–1071. ISSN 0196-8904.
- [41] SORRENTINO, Giancarlo et al. Influence of preheating and thermal power on cyclonic burner characteristics under mild combustion. *Fuel*. 2018, Vol. 233, pp. 207–214. ISSN 0016-2361.
- [42] HUANG, Mingming et al. Effect of air preheat temperature on the MILD combustion of syngas. *Energy Conversion and Management*. 2014, Vol. 86, pp. 356–364. ISSN 0196-8904.
- [43] GUPTA, Ashwani K.; BOLZ, S.; HASEGAWA, T. Effect of Air Preheat Temperature and Oxygen Concentration on Flame Structure and Emission. *Journal of Energy Resources Technology*. 1999, Vol. 121, pp. 209–216. ISSN 0195-0738
- [44] Burner testing facility. In: *Institute of Process Engineering*. [online]. Retrieved 2018-07-22. Available from: <http://www.upei.fme.vutbr.cz/en/research/burner-testing-facility>
- [45] KERMES, Vít et al. Testing of gas and liquid fuel burners for power and process industries. *Energy*. 2008, Vol. 33, pp. 1551–1561. ISSN 0016-2361.
- [46] BĚLOHRADSKÝ, Petr. *Metody pro určování charakteristických procesů spalování na bázi experimentů a modelování*. Brno: Vysoké učení technické v Brně, Fakulta strojního inženýrství, 2010. 143 p. Supervisor of the Doctoral Thesis: prof. Ing. Petr Stehlík, CSc.
- [47] Plynové hořáky APH - M(E). In: *PBS Power Equipment*. [online]. Retrieved 2018-09-28. Available from: [http://www.pbspe.cz/cze/index.php?action=catalogue\\_detail&id=29](http://www.pbspe.cz/cze/index.php?action=catalogue_detail&id=29)
- [48] HUDÁK, Igor. *Předehřev spalovacího vzduchu – Technická zpráva*. Brno: Vysoké učení technické v Brně. [internal document].
- [49] MACENAUEROVÁ, Tereza. *Vliv vnitřní recirkulace spalin na charakteristické parametry spalování*. Brno: Vysoké učení technické v Brně, Fakulta strojního inženýrství, 2015. 58 p. Supervisor of the master's thesis: Ing. Petr Bělohradský, Ph.D.
- [50] 3D models of the burners. Vysoké učení technické v Brně. [internal document].
- [51] HUDÁK, Igor. *Charakteristické parametry procesu spalování při využití vzduchu s obsahem kyslíku vyšším než 21 %*. Brno: Vysoké učení technické v Brně, Fakulta strojního inženýrství, 2013. 44 p. Supervisor of the master's thesis: Ing. Petr Bělohradský, Ph.D.
- [52] BAŠTA, Jiří. *Otopné plochy – otopná tělesa*. 2<sup>nd</sup> ed., Praha: České vysoké učení technické v Praze, 2016. 204 p. ISBN 978-80-01-05943-2.

- [53] Kvalita plynu. In: *GasNet, člen innogy*. [online]. Retrieved 2018-09-29. Available from: <https://www.gasnet.cz/cs/kvalita-plynu>
- [54] API Standard 560: Fired Heaters for General Refinery Service. 5<sup>th</sup> ed., American Petroleum Institute, 2016. 327 p.